

NASA Technical Memorandum 86364

**Low-Speed Wind-Tunnel
Tests of an Advanced
Eight-Bladed Propeller**

**Paul L. Coe, Jr., Garl L. Gentry, Jr.,
and Dana Morris Dunham**

*Langley Research Center
Hampton, Virginia*



National Aeronautics
and Space Administration

Scientific and Technical
Information Branch

1985

Contents

Summary	1
Introduction	1
Symbols	1
Model	2
Tests	2
Results and Discussion	2
Comparison With Other Data	2
Propeller Performance Characteristics ($\alpha = 0^\circ$)	3
Effect of Angle of Attack on Propeller Performance Characteristics	3
Effect of Angle of Attack on Propeller Force and Moment Characteristics	3
Summary of Results	4
References	4
Table	5
Figures	6
Appendix A—Nondimensional Power Loading	29
Appendix B—Propeller Force and Moment Characteristics	30
Propeller Normal-Force Coefficient	30
Propeller Pitching-Moment Coefficient	30
Appendix C—Data Supplement	34

PAGE THREE OF THE BLANK NOT FILMED

Summary

As part of a research program on advanced turboprop aircraft aerodynamics, a low-speed wind-tunnel investigation was conducted to document the basic performance and force/moment characteristics of an advanced eight-bladed propeller. The results show that in addition to the normal force and pitching moment produced by the propeller/nacelle combination at angle of attack, a significant side force and yawing moment are also produced. Furthermore, it is shown that for test conditions wherein compressibility effects can be ignored, accurate simulation of propeller performance and flow fields can be achieved by matching the nondimensional power loading of the model propeller to that of the full-scale propeller.

Introduction

Several studies have identified potentially significant fuel savings for advanced turboprop aircraft. (See, for example, ref. 1.) The results of these studies indicate that wing- and aft-mounted advanced turboprop configurations appear feasible and that configuration selection will depend on further information regarding acoustic-treatment requirements, structural weight, and engine/airframe installation aerodynamics. Although decades of experience exist for propeller-driven aircraft, this experience has been for configurations having significantly lower power loadings than those presently considered. Besides the question of performance and efficiency, a major uncertainty associated with the aerodynamic characteristics of advanced turboprop aircraft configurations is the lack of information regarding the impact of the highly disk loaded turboprop installation on aircraft stability and control during the takeoff, climb, and approach phases of flight.

The investigation discussed herein is part of a broad NASA research program to obtain fundamental aerodynamic information regarding advanced turboprop installation effects. This investigation was conducted to provide baseline information regarding the performance and force/moment characteristics of an isolated turboprop/nacelle combination operating over a range of angles of attack from 0° to 20° , a range of advance ratios from 0.4 to 2.5, and a range of blade angles from -1.08° to 42.27° . The tests were conducted in the Langley 4- by 7-Meter Tunnel for a range of Reynolds numbers (based on blade chord) of 0.15×10^6 to 0.48×10^6 and a range of Mach numbers from 0.05 to 0.14. Appendixes A, B, and C provide additional information on the nondimensional power loading and propeller force and moment characteristics with a data supplement on the test program.

Symbols

All data have been reduced to coefficient form and are presented in the body axis system. (See fig. 1.) Computer symbols used are given in parentheses.

C_m	(CPM)	pitching-moment coefficient, $M_Y/q_\infty Sd$
C_N	(CNF)	normal-force coefficient, $F_N/q_\infty S$
C_n	(CYM)	yawing-moment coefficient, $M_Z/q_\infty Sd$
C_P	(CP)	power coefficient, $P/\rho n^3 d^5$ $= 2\pi C_Q$
C_Q		torque coefficient, $Q/\rho n^2 d^5$
C_T	(CT)	thrust coefficient, $T/\rho n^2 d^4$
C_Y	(CSF)	side-force coefficient, $F_Y/q_\infty S$
d		propeller diameter, ft
F_N		normal force, lbf
F_Y		side force, lbf
J	(J)	advance ratio, V_∞/nd
ℓ		distance from propeller pitch change axis to balance moment reference center, ft
M_Y		pitching moment, ft-lbf
M_Z		yawing moment, ft-lbf
n		propeller rotational speed, rps
P		power, hp
Q		torque (balance rolling moment), ft-lbf
q		local dynamic pressure, psf
q_∞		free-stream dynamic pressure, psf
R		Reynolds number based on blade chord and velocity at 0.75r station
r		propeller radius, ft
S		propeller disk area, ft^2
T		thrust force (negative balance axial force), lbf
T_c		thrust disk-loading coefficient, $T/\rho V_\infty^2 d^2$
V_∞		free-stream velocity, ft/sec

x	distance measured aft of spinner nose, in.
α	(ALPHA) angle of attack, deg
$\beta_{.75}$	blade angle defined at 0.75r station
η	propeller efficiency, $J C_T / C_P$
ξ	distance from point of application of nacelle normal force to balance moment reference center, ft
ρ	free-stream density, slugs/ft ³
Subscripts:	
meas	value measured with propeller operating
nac	force or moment acting on nacelle
prop	force or moment acting on propeller
prop off	value measured for isolated nacelle

Model

The dimensional characteristics of the propeller and nacelle used in this investigation are listed in table I and shown in figure 2. A photograph showing the model mounted for tests in the Langley 4- by 7-Meter Tunnel is presented in figure 3.

The propeller model tested was an eight-bladed aluminum SR-2 design with a 1.408-ft diameter. The planform and twist distribution for the SR-2 propeller are well documented in reference 2. The propeller was powered by a 29-hp (at 10 000 rpm) electric motor, as sketched in figure 2.

Tests

The model was tested over an angle-of-attack range from 0° to 20° for blade angles $\beta_{.75}$ of -1.08°, 20.59°, 25.52°, 30.45°, and 42.27°. Tests were conducted for the wind tunnel configured with both open and closed test sections for dynamic pressures q ranging from 4.5 to 28 psf. A description of the wind tunnel is provided in references 3 and 4.

The propeller advance ratio was varied from 0.4 to approximately 2.5. The combination of propeller rotational speed and tunnel free-stream velocity resulted in a range of Reynolds numbers R (based on the blade chord) from 0.15×10^6 to 0.48×10^6 . Forces

and moments were measured with a standard six-component strain-gauge balance mounted internally to the nacelle, as indicated in figure 2.

Wake velocity measurements were made with a pressure rake (see fig. 4) consisting of seven parallel (five-hole) probes mounted such that they were aligned with the nacelle, and measurements were taken at a longitudinal station 5.0 in. aft of the propeller pitch change axis. The innermost probe was located at a lateral station 5.0 in. from the nacelle centerline, and the spacing between individual probe centerlines was 2.0 in.

Alternative, nonintrusive velocity measurements were made by using a laser velocimeter (LV). (See ref. 5 for a complete description of the LV system.) The four-beam LV is capable of measuring two velocity components simultaneously. The axial and radial components are obtained by making measurements in the vertical plane that passes through the propeller/nacelle axis. Flow measurements were made at three stations: 1.25 in. ahead of the propeller pitch change axis and 1.25 and 5.0 in. aft of the propeller pitch change axis.

Results and Discussion

As noted previously, the 1.408-ft-diameter propeller tested was powered by a 29-hp (at 10 000 rpm) electric motor. This combination results in a maximum power loading P/d^2 of 14.62 hp/ft². It is recognized that the advanced turboprop concepts currently under consideration operate with considerably higher values of power loading. However, by matching the propeller characteristics in coefficient form, the present tests simulate high-power-loading advanced turboprop concepts. Specifically, appendix A shows that the appropriate parameter to match for accurate simulation is the nondimensional power loading $P/d^2 q_{\infty} V_{\infty}$.

It should be noted that the forces and moments measured in this test reflect the combined loads of both the propeller and the nacelle. However, tests conducted with the isolated nacelle (blades off) show that the axial force and rolling moment attributed to the nacelle are negligible in the calculation of C_T and C_P . Therefore, the thrust and power coefficients presented in subsequent discussions can be considered as a reasonable measure of propeller performance.

A run schedule and tabular listing of the data are contained in the data supplement presented as appendix C.

Comparison With Other Data

Power constraints, imposed by the electric motor, required that the low values of advance ratio

$(J = V_\infty/nd)$ be achieved by reducing tunnel velocity. Consequently, a blade angle setting of $\beta_{.75} = 30.45^\circ$ was selected and tests were conducted to determine the effect of tunnel velocity on the propeller performance characteristics for angles of attack of 0° and 8° . These results are presented in figures 5 and 6 for the tunnel configured with closed and open test sections, respectively. Examination of the results indicates that there is no discernible influence of tunnel velocity and that identical results are obtained with either the closed or open test section. To confirm the blade design and balance results, comparisons were made with data for a larger eight-bladed steel SR-2 propeller ($d = 2.042$ ft) provided by the Lewis Research Center. (Ref. 6 describes the Lewis tests but does not include the data provided herein.) Figure 7 presents a representative comparison of the Lewis data with data from the present tests for a nominal value of $\beta_{.75} = 30^\circ$. As shown, agreement between the two data sets is excellent.

Propeller Performance Characteristics ($\alpha = 0^\circ$)

Figure 8 presents the variation of propeller thrust and power coefficients as a function of advance ratio. Data are presented for blade angles of -1.08° , 20.59° , 25.52° , 30.45° , and 42.27° . For the $\beta_{.75} = -1.08^\circ$ condition, the propeller characteristics closely resemble those of a flat disk normal to the free stream, and the power or torque required is seen to be relatively small and approximately constant with respect to advance ratio.

Effect of Angle of Attack on Propeller Performance Characteristics

Figure 9 shows the effect of angle of attack on the propeller performance characteristics for $\beta_{.75} = 20.59^\circ$, 25.52° , 30.45° , and 42.27° . From noting that the advance ratio is defined as $J = V_\infty/nd$ and that the axial component of velocity is $V_\infty \cos \alpha$ for propellers at angle of attack, the performance characteristics are plotted as a function of $J \cos \alpha$ in figure 10. As can be seen, the thrust and power coefficients nearly collapse to a single curve when plotted against $J \cos \alpha$. This result has been well established (see, for example, ref. 7) for more conventional propellers.

Effect of Angle of Attack on Propeller Force and Moment Characteristics

Figure 11 presents the pitching-moment, yawing-moment, normal-force, and side-force coefficients as a function of advance ratio at angles of attack of 0° , 8° , 16° , and 20° for $\beta_{.75} = 30.45^\circ$. These coefficients are for the combined propeller and nacelle

assembly and are measured about the moment reference center shown in figure 2. The normal-force data show considerable scatter for the low load conditions (i.e., $\alpha < 16^\circ$). Most significantly, the data show that yawing moments and side forces substantially greater than those predicted by classical propeller theory are produced by the propeller/nacelle combination at angle of attack. Although the data presented are insufficient to determine the origin of this result, later laser velocimeter measurements indicate that this result stems from the interaction of the propeller slipstream with the nacelle flow field. This interaction originates from the fact that the downgoing blade of a propeller disk at angle of attack experiences an increased blade-section angle of attack and, consequently, produces an increased thrust relative to the upgoing blade. Thus, for angle-of-attack conditions, the pressure increase across the downgoing side of the propeller disk is greater than that on the upgoing side, with the outcome that a crossflow is produced on the nacelle. This nacelle crossflow causes a side force and yawing moment.

Isolating the propeller force and moment characteristics from those measured for the propeller/nacelle combination requires either a separate propeller balance or knowledge of the isolated nacelle characteristics with detailed information regarding the nacelle flow field. Appendix B presents an approximate analysis (based on the data of figs. 11, 12, and 13) to determine the contribution of the isolated propeller to the measured normal-force and pitching-moment characteristics. Figure 12 shows the variation of pitching moment and normal force with angle of attack for the isolated nacelle (propeller blades off), and figure 13 illustrates the dynamic pressure ratio of the flow over the nacelle (aft of the propeller disk) as a function of advance ratio.

Velocity distributions behind the propeller were calculated from both the LV and pressure-probe data. Figure 14 presents the nondimensional axial, radial, and circumferential velocities (as determined from laser velocimeter measurements) as a function of the nondimensional radial distance from the nacelle centerline. The axial measurement stations correspond to 0.25 in. ahead of and behind the propeller blades (1.25 in. forward and aft of the propeller pitch change axis) and 5.0 in. aft of the propeller pitch change axis. The data illustrate the expected trend of increasing axial velocity with increasing distance downstream of the propeller and of negligible radial velocities, except in the vicinity of the spinner just forward of the blades. The data further show circumferential velocities ahead of the propeller disk that also increase downstream of the propeller. Calculations show that the swirl angle correspondingly in-

creases downstream; for example, at $r/R = 0.78$ the swirl increases from 6.5° just ahead of the blades to 8.3° just aft of the blades and 10.2° at 5.0 in. downstream of the propeller pitch change axis. Figure 15 presents a comparison of the aforementioned velocity ratios with those based on pressure probe measurements. As can be seen, the results from the pressure probe are in fair agreement for the axial and radial velocity components. However, the circumferential velocities, as determined from the pressure probe, are substantially below those values based on laser velocimeter measurements. The reason for this discrepancy has not been determined.

Summary of Results

The results of low-speed wind-tunnel tests to determine basic performance and force/moment characteristics of an advanced eight-bladed propeller may be summarized as follows:

1. The propeller thrust and power coefficients C_T and C_P , when plotted as a function of advance ratio J , exhibit a parametric dependence on angle of attack α . However, this dependence can be taken into account by considering C_T and C_P plotted against $J \cos \alpha$.
2. In addition to the normal force and pitching moment produced by the propeller/nacelle combination at angle of attack, the data show that significant yawing moments and side forces are produced.
3. For test conditions wherein compressibility effects can be ignored, accurate simulation of propeller performance and flow fields can be achieved

by matching the nondimensional power loading of the model propeller to that of the full-scale propeller.

NASA Langley Research Center
Hampton, VA 23665
March 27, 1985

References

1. Goldsmith, I. M.: *A Study To Define the Research and Technology Requirements for Advanced Turbo/Propfan Transport Aircraft*. NASA CR-166138, 1981.
2. Jeracki, Robert J.; Mikkelsen, Daniel C.; and Blaha, Bernard J.: *Wind Tunnel Performance of Four Energy Efficient Propellers Designed for Mach 0.8 Cruise*. NASA TM-79124, 1979.
3. Applin, Zachary T.: *Flow Improvements in the Circuit of the Langley 4- by 7-Meter Tunnel*. NASA TM-85662, 1983.
4. Block, P. J. W.; and Gentry, Garl L., Jr.: *Evaluation of the Langley 4- by 7-Meter Tunnel for Propeller Noise Measurements*. NASA TM-85721, 1984.
5. Hoad, Danny R.; Rhodes, David B.; and Meyers, James F.: *Preliminary Rotor Wake Measurements With a Laser Velocimeter*. NASA TM-83246, AVRADCOM TR 82-B-7, 1983.
6. Stefko, George L.; Bober, Lawrence J.; and Neumann, Harvey E.: *New Test Techniques and Analytical Procedures for Understanding the Behavior of Advanced Propellers*. NASA TM-83360, [1983].
7. De Young, John: *Propeller at High Incidence*. *J. Aircr.*, vol. 2, no. 3, May-June 1965, pp. 241-250.
8. Ribner, Herbert S.: *Propellers in Yaw*. NACA Rep. 820, 1945. (Supersedes NACA ARR 3L09.)

TABLE I. DIMENSIONAL CHARACTERISTICS

(a) Overall geometric characteristics

Propeller diameter, ft	1.408
Propeller disk area, ft ²	1.558
Maximum nacelle diameter, ft	0.5
Overall length, ft	3.61
Distance of moment reference center aft of propeller disk, ft	2.95

(b) Nacelle ordinates

<i>x</i> , in.	<i>r</i> , in.
0	0
.270	.340
.440	.480
.780	.710
1.110	.920
1.810	1.230
2.510	1.500
3.220	1.730
3.890	1.870
4.640	1.930
5.040	2.020
5.600	2.210
6.230	2.450
6.600	2.580
6.617	2.581
6.738	2.619
6.876	2.665
7.014	2.707
7.152	2.745
7.290	2.778

<i>x</i> , in.	<i>r</i> , in.
7.703	2.859
8.393	2.945
9.428	2.997
10.000	3.000
:	:
29.000	3.000
30.000	2.940
31.000	2.900
32.000	2.850
33.000	2.520
34.000	2.300
35.000	2.160
36.000	2.020
37.000	1.920
38.000	1.820
39.000	1.750
40.000	1.680
41.000	1.620
42.000	1.600
43.000	1.560
43.317	1.550

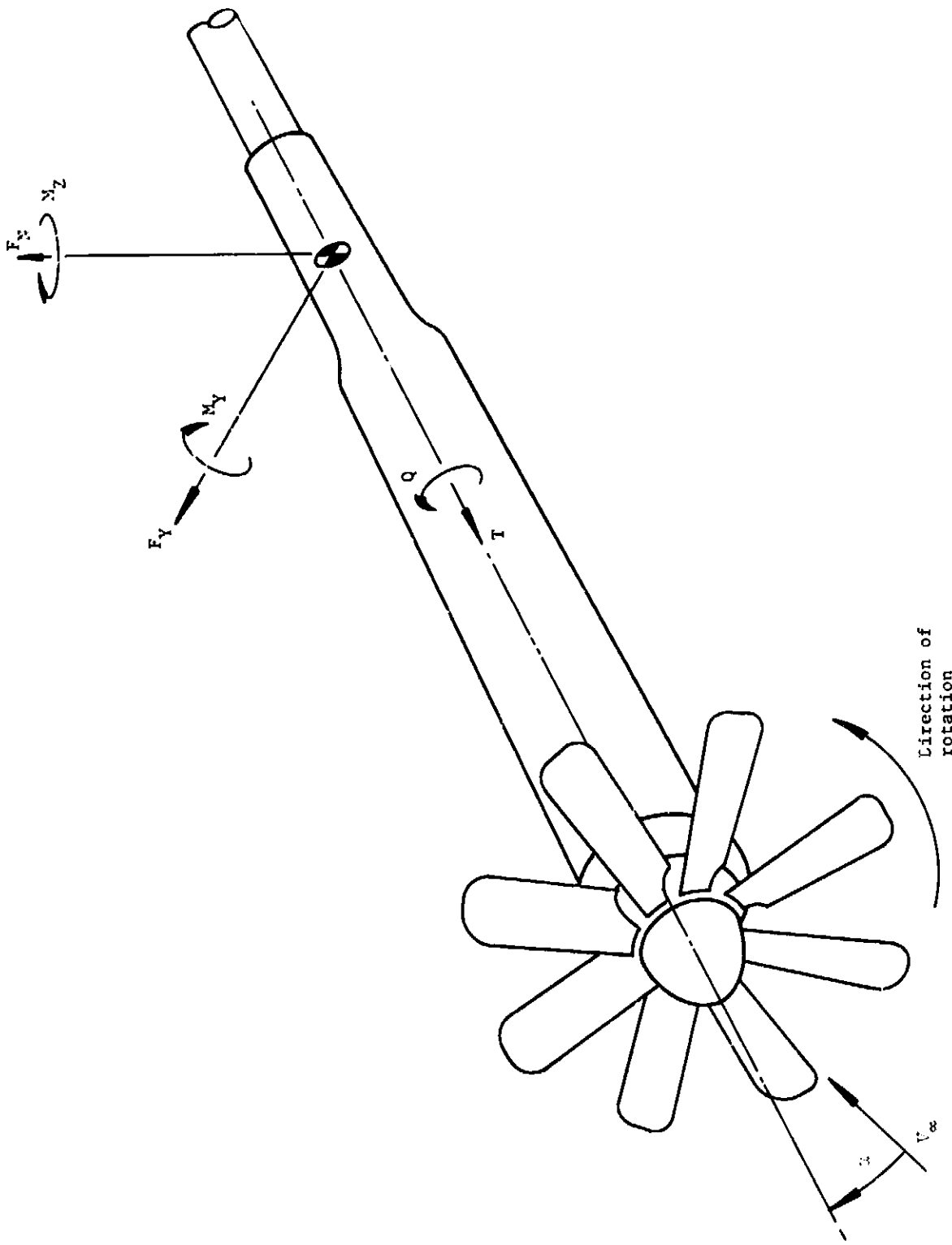


Figure 1. Sketch of propeller and nacelle showing body system of axes.

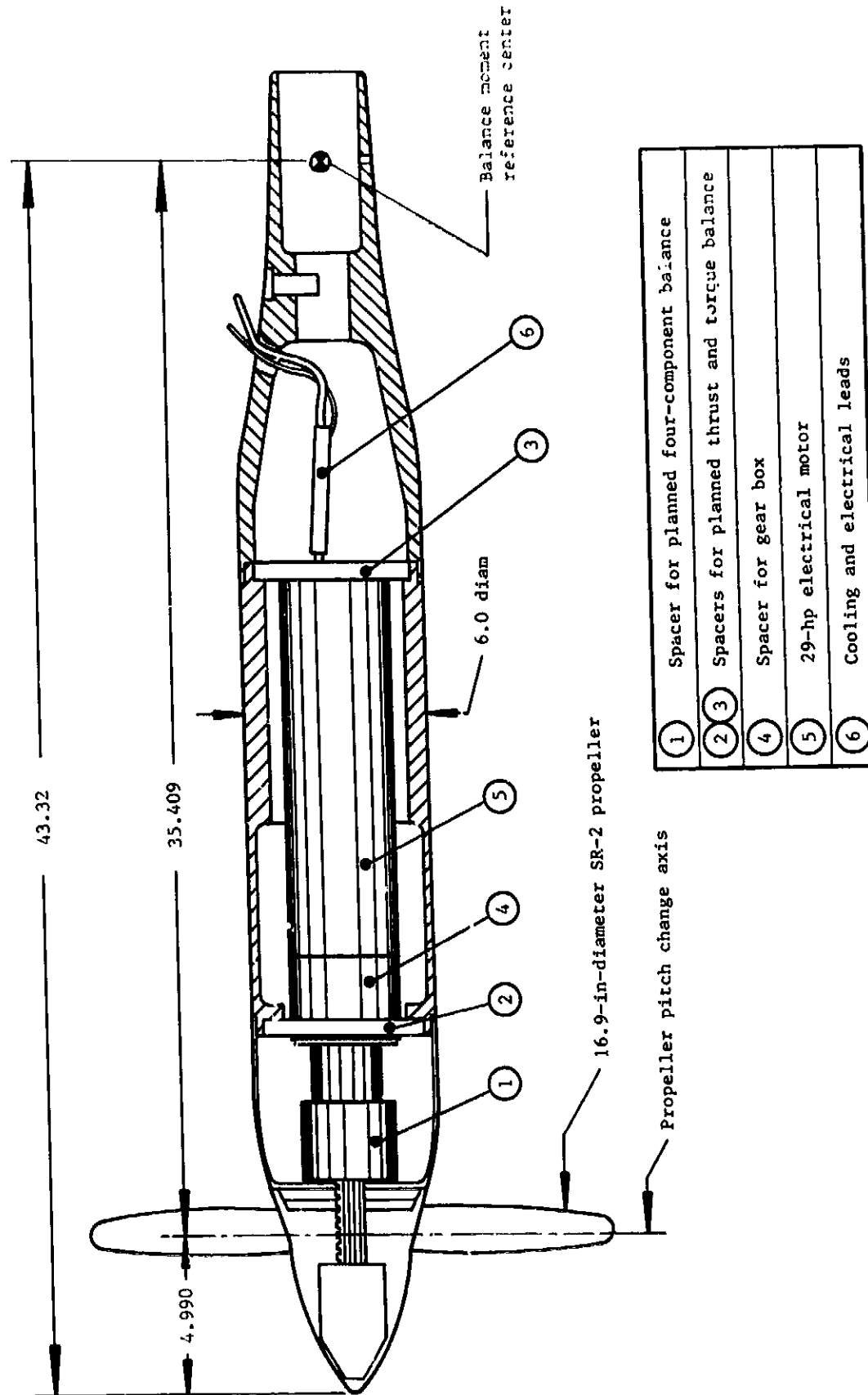
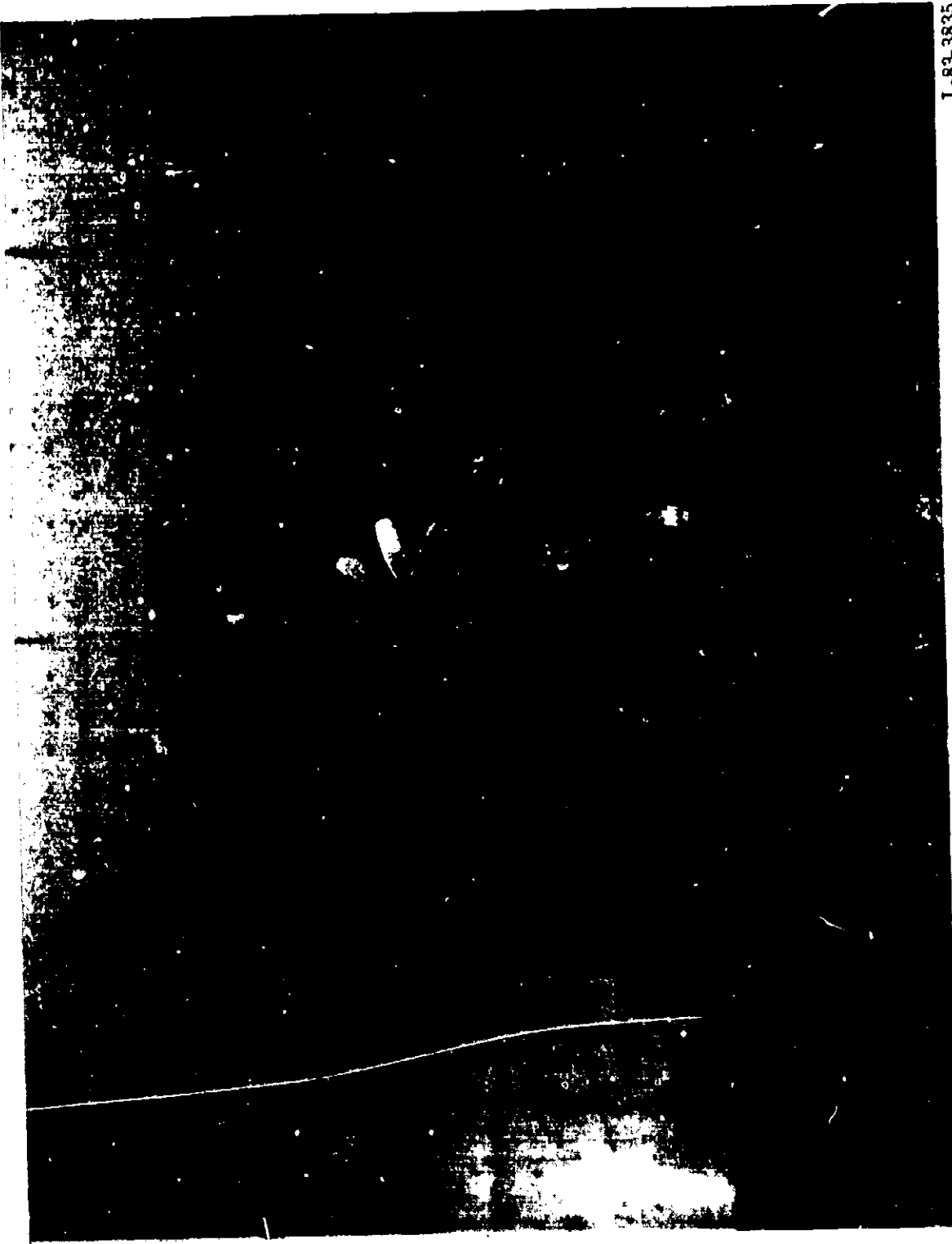
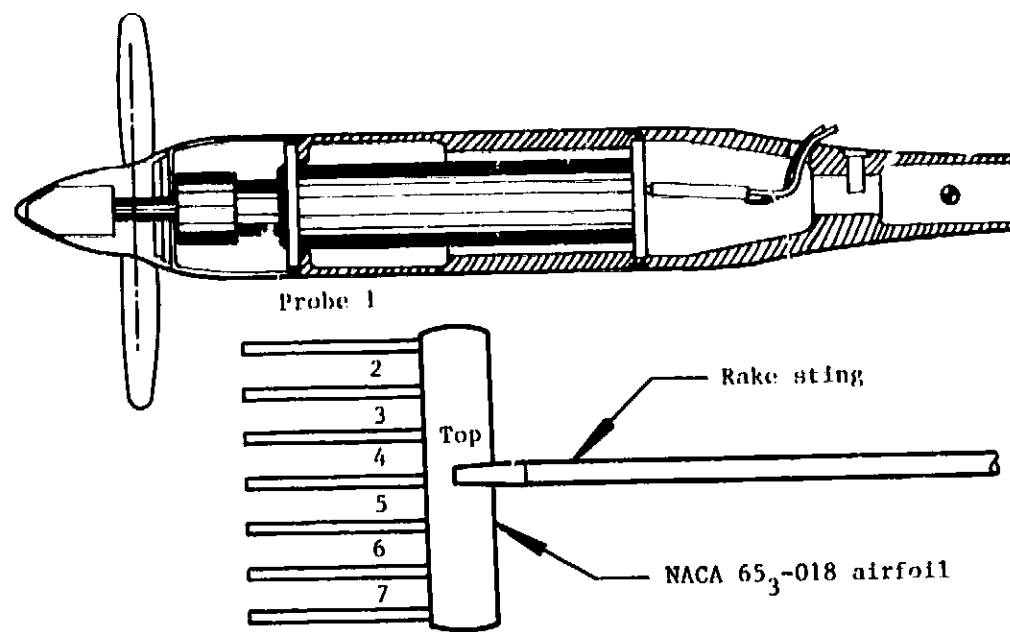


Figure 2. Sketch of propeller/nacelle combination. All dimensions are given in inches.

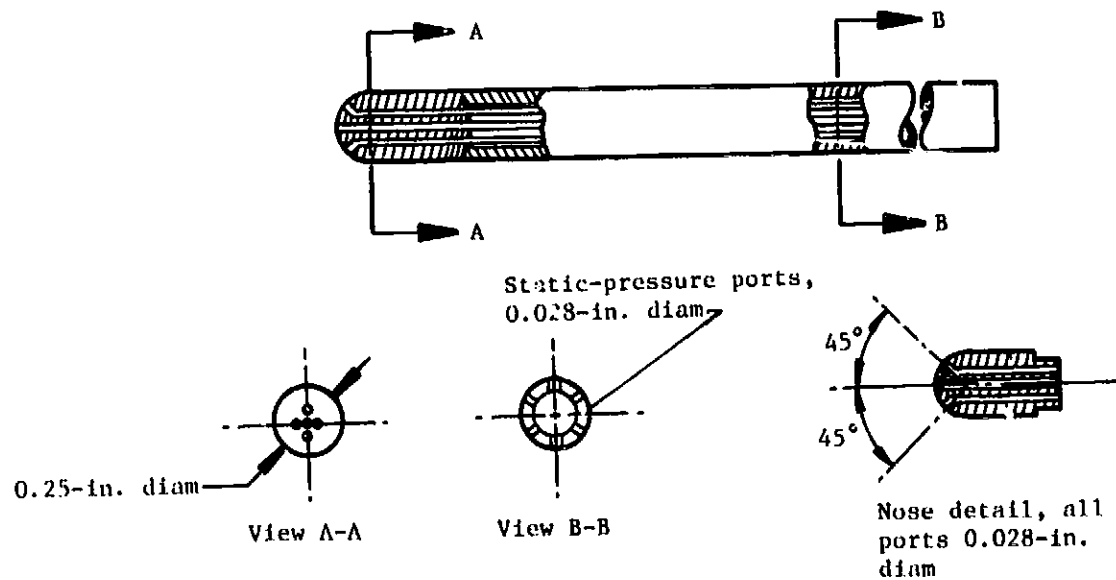
ADVANCED PROPELLER
OF POOR QUALITY



L-83-3835
Figure 3. Advanced eight-bladed propeller/nacelle combination mounted for tests in the Langley 4-by 7-Meter Tunnel.



(a) Sketch of pressure rake.



(b) Probe details.

Figure 4. Sketches of pressure rake and probe details.

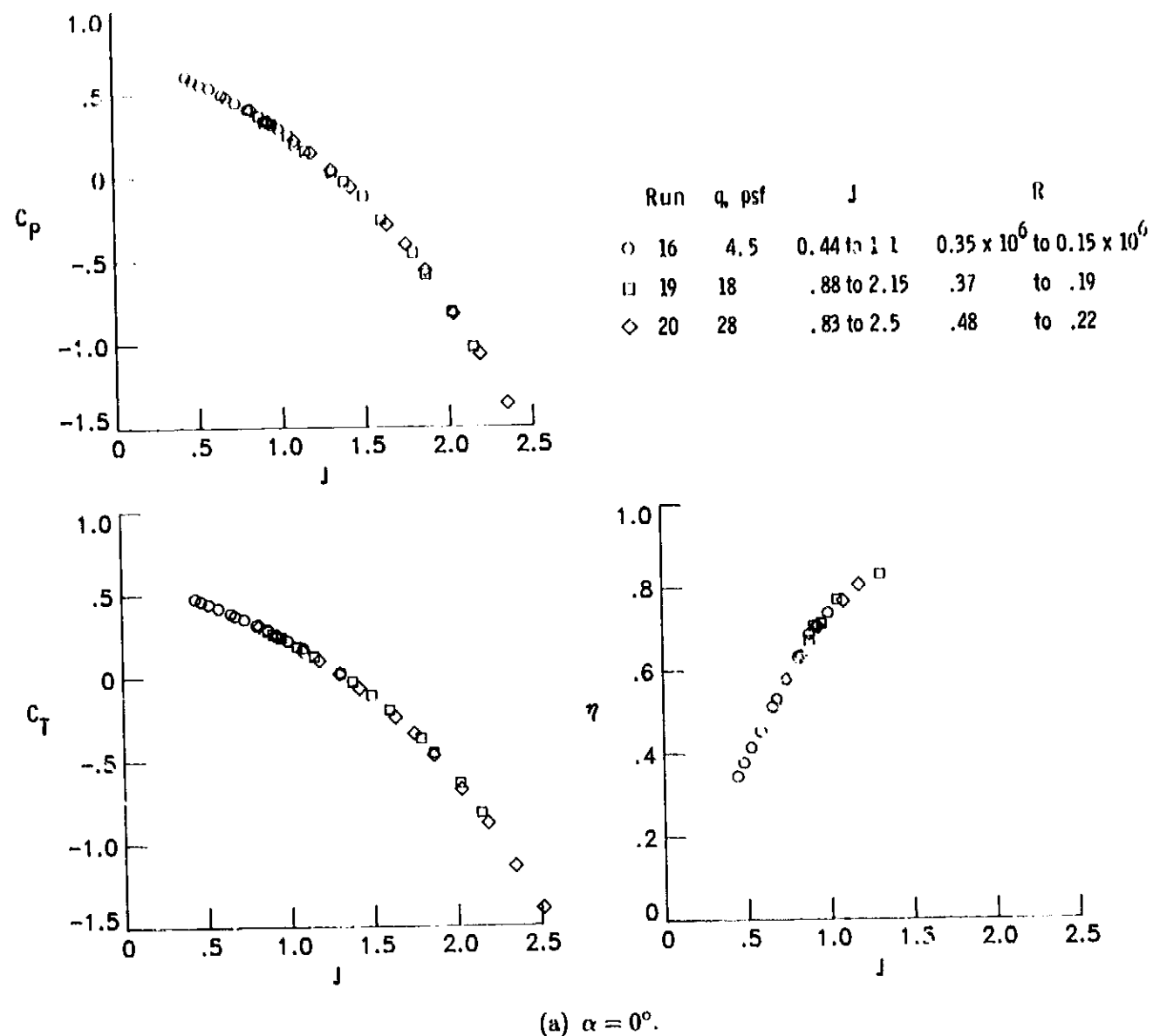
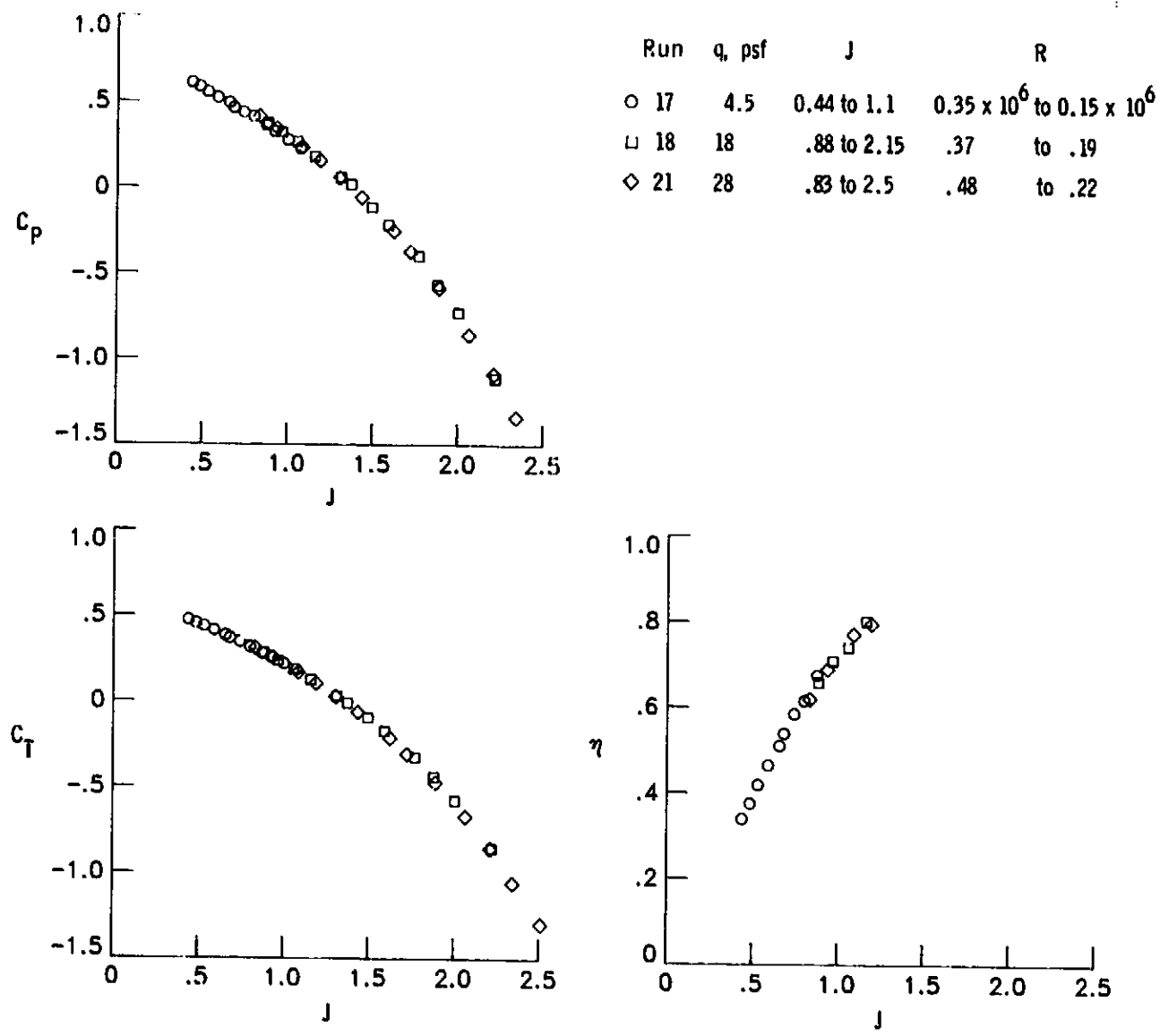
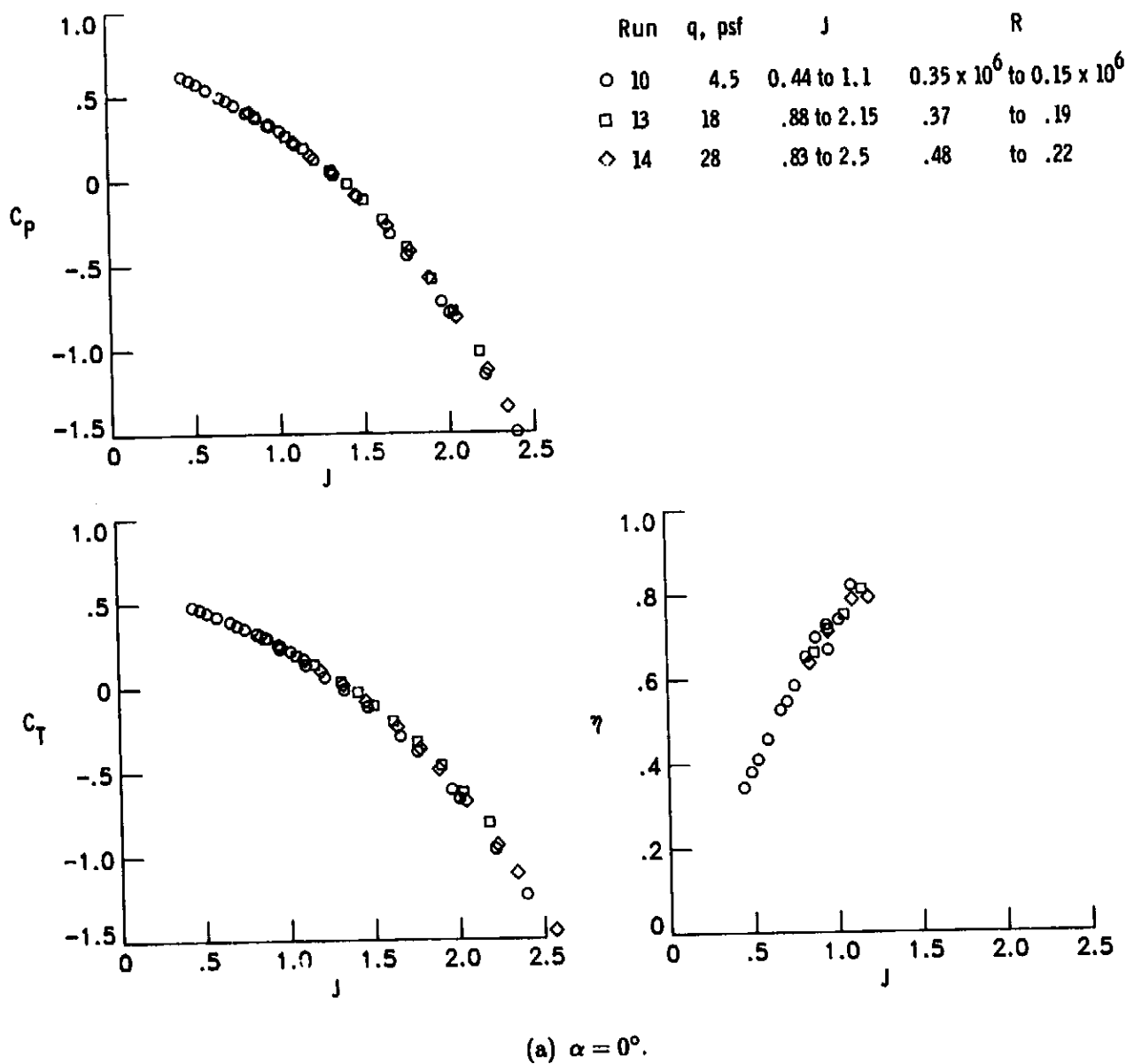


Figure 5. Effect of dynamic pressure on propeller performance characteristics in closed test section.
 $\beta_{.75} = 30.45^\circ$.



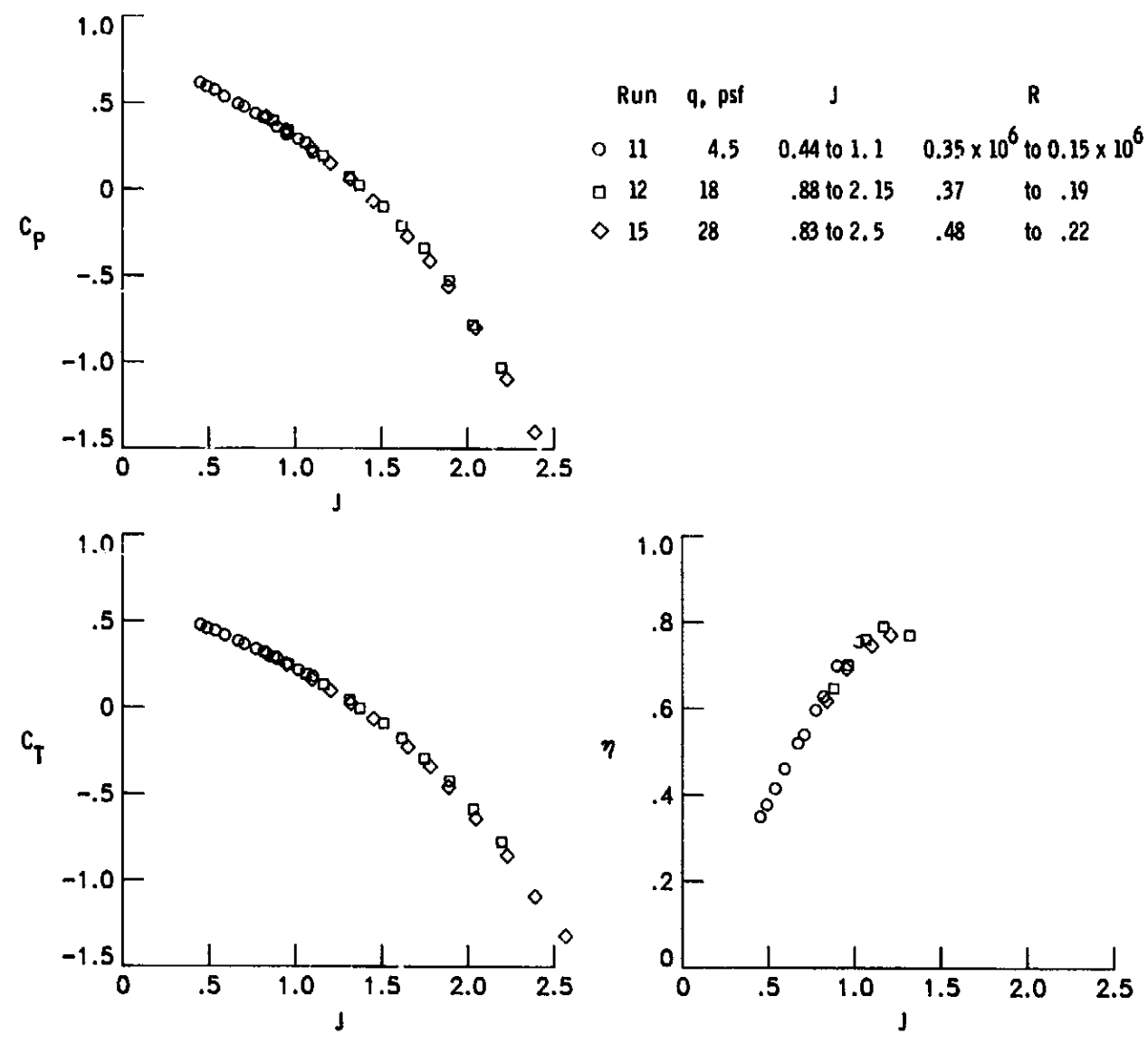
(b) $\alpha = 8^\circ$.

Figure 5. Concluded.



(a) $\alpha = 0^\circ$.

Figure 6. Effect of dynamic pressure on propeller performance characteristics in open test section.
 $\beta_{.75} = 30.45^\circ$.



(b) $\alpha = 8^\circ$.

Figure 6. Concluded.

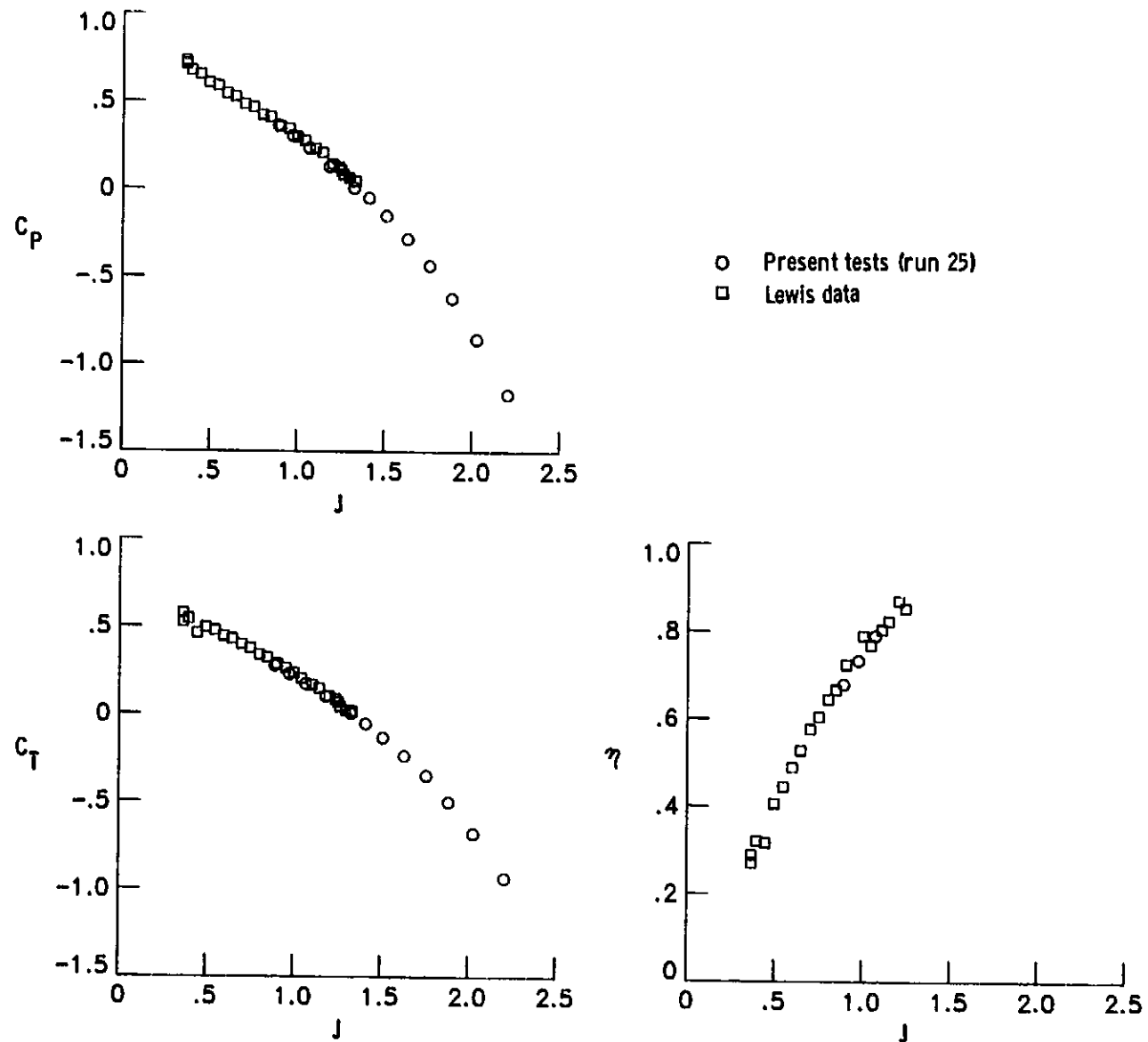


Figure 7. Comparison of data from present tests with data provided by the Lewis Research Center. $\beta_{.75} = 30^\circ$.

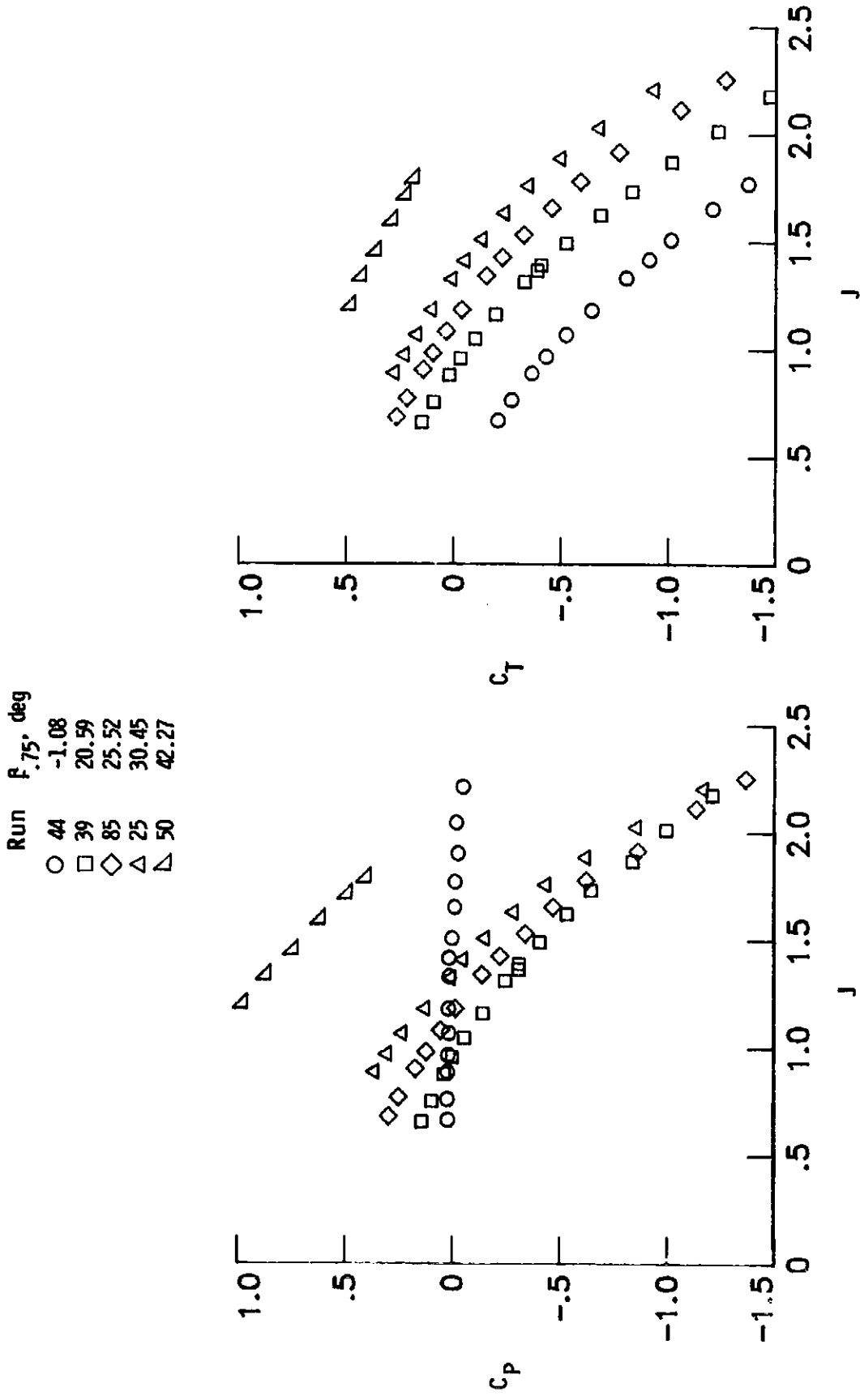
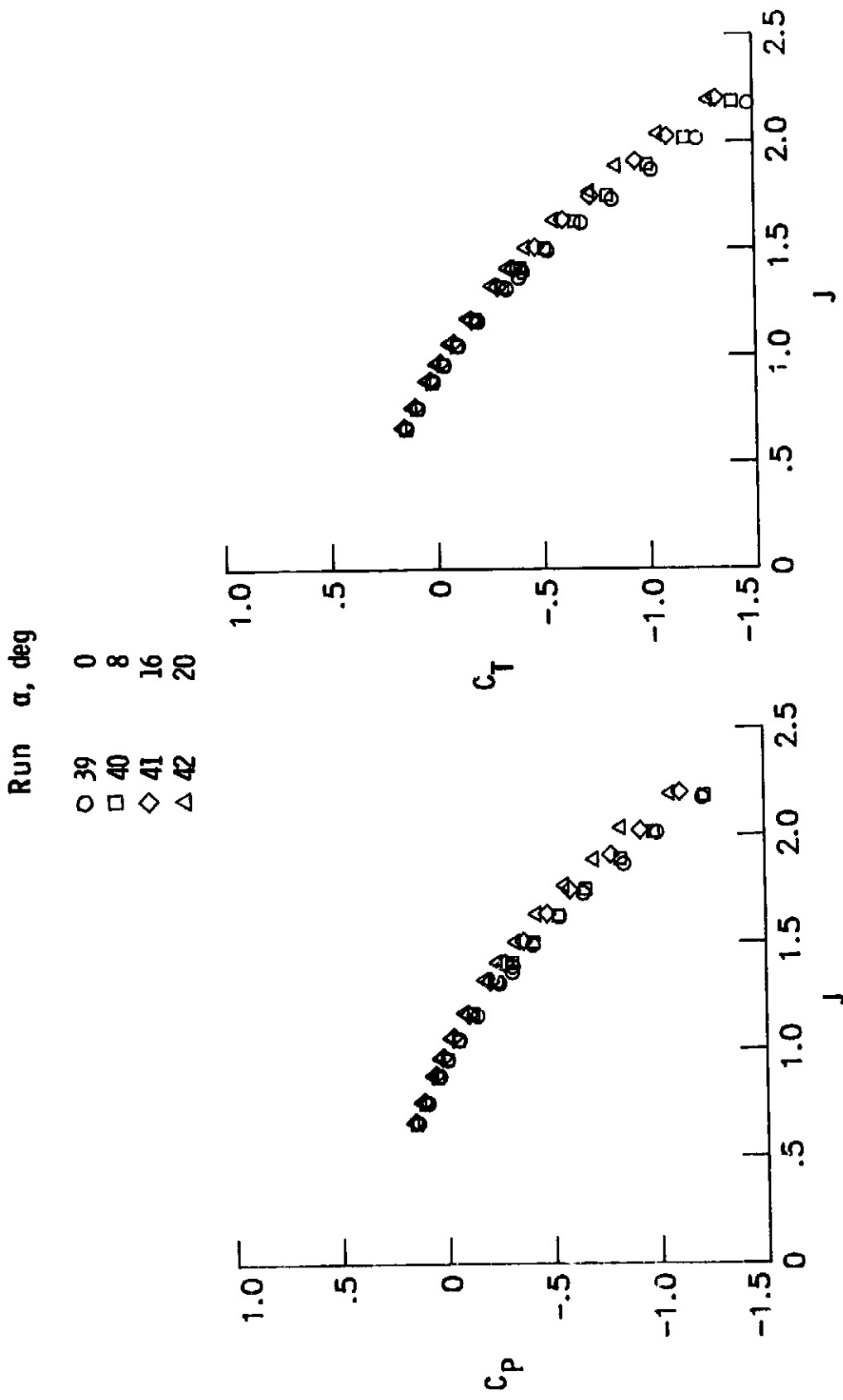
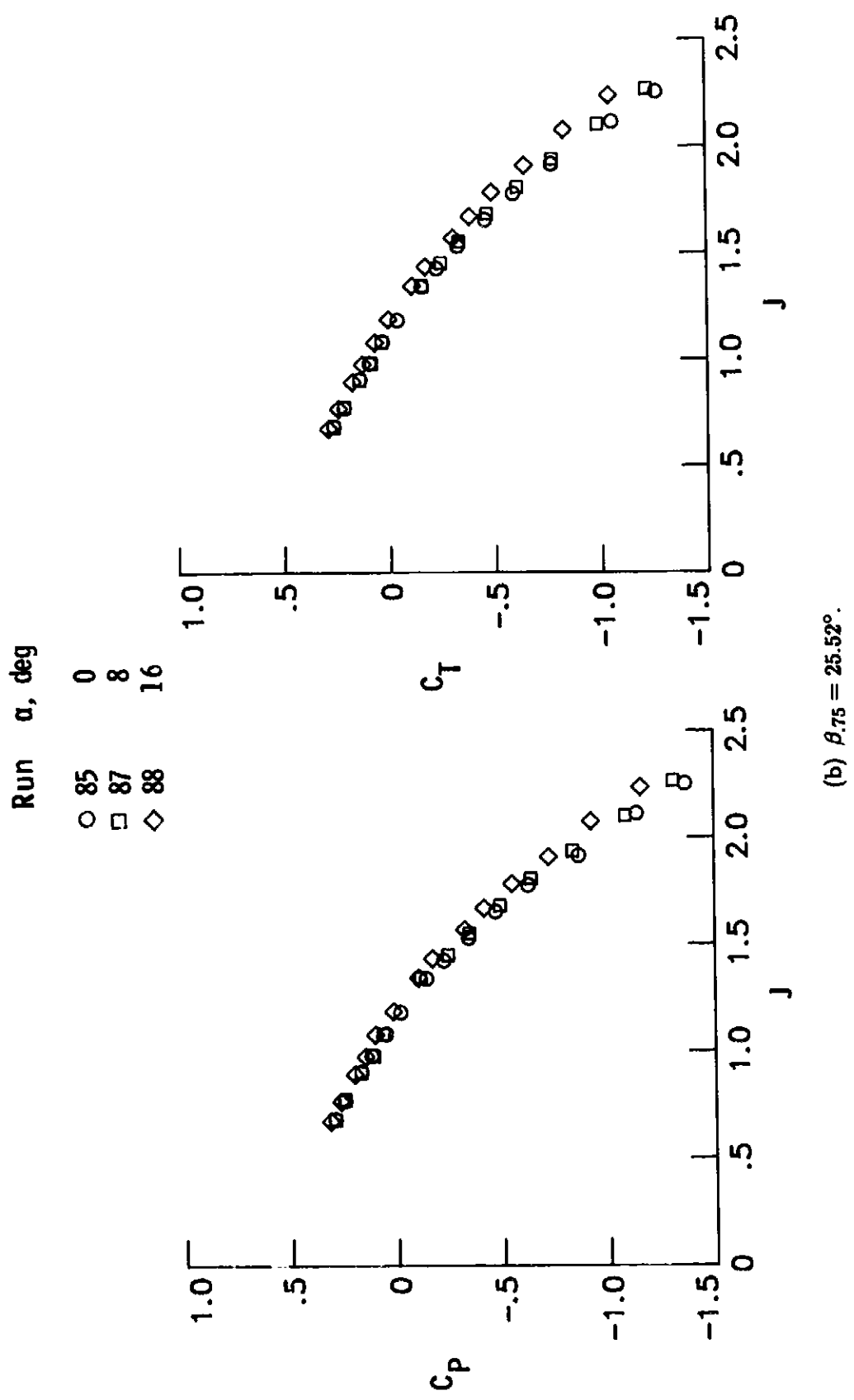


Figure 8. Propeller performance characteristics.



(a) $\beta_{75} = 20.59^\circ$.

Figure 9. Effect of angle of attack on propeller performance.

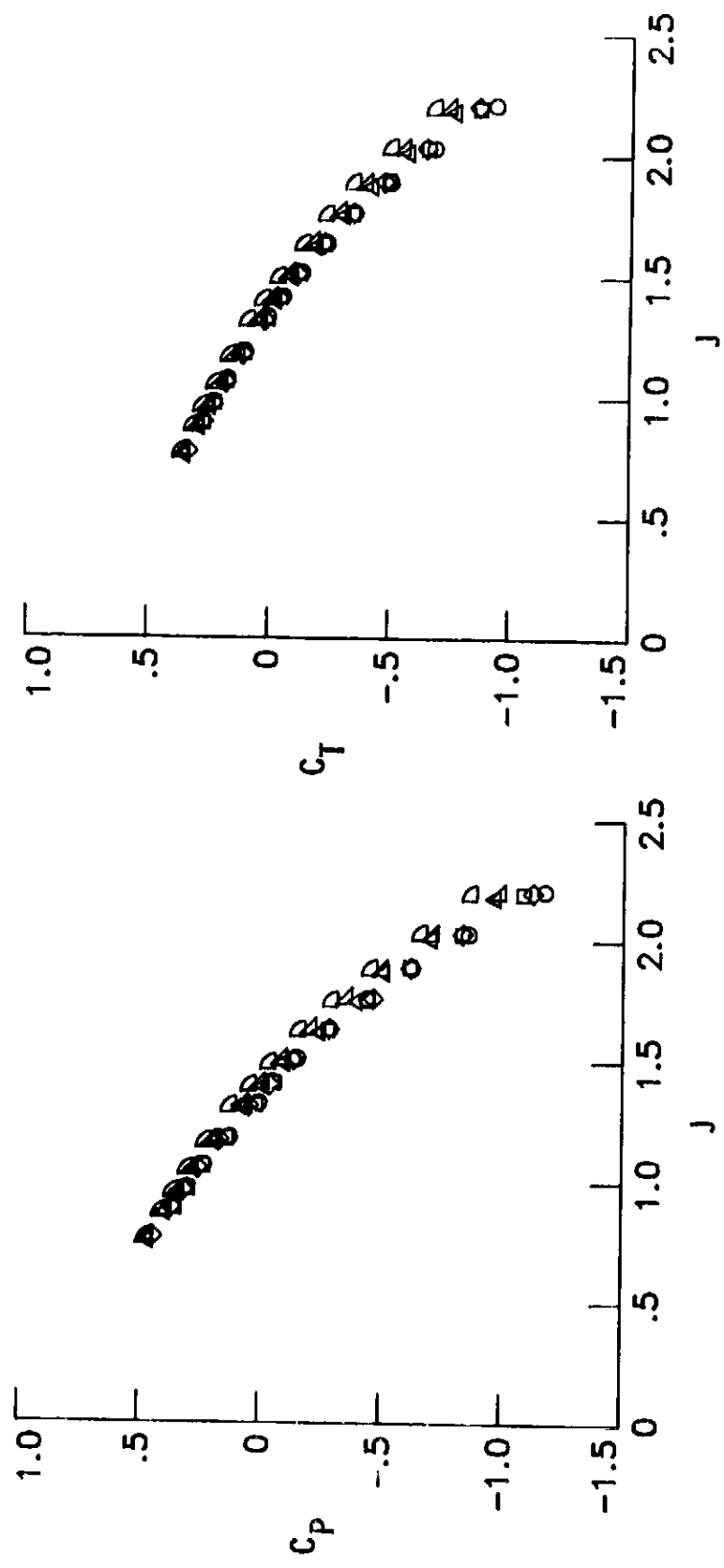


(b) $\beta_{75} = 25.52^\circ$.

Figure 9. Continued.

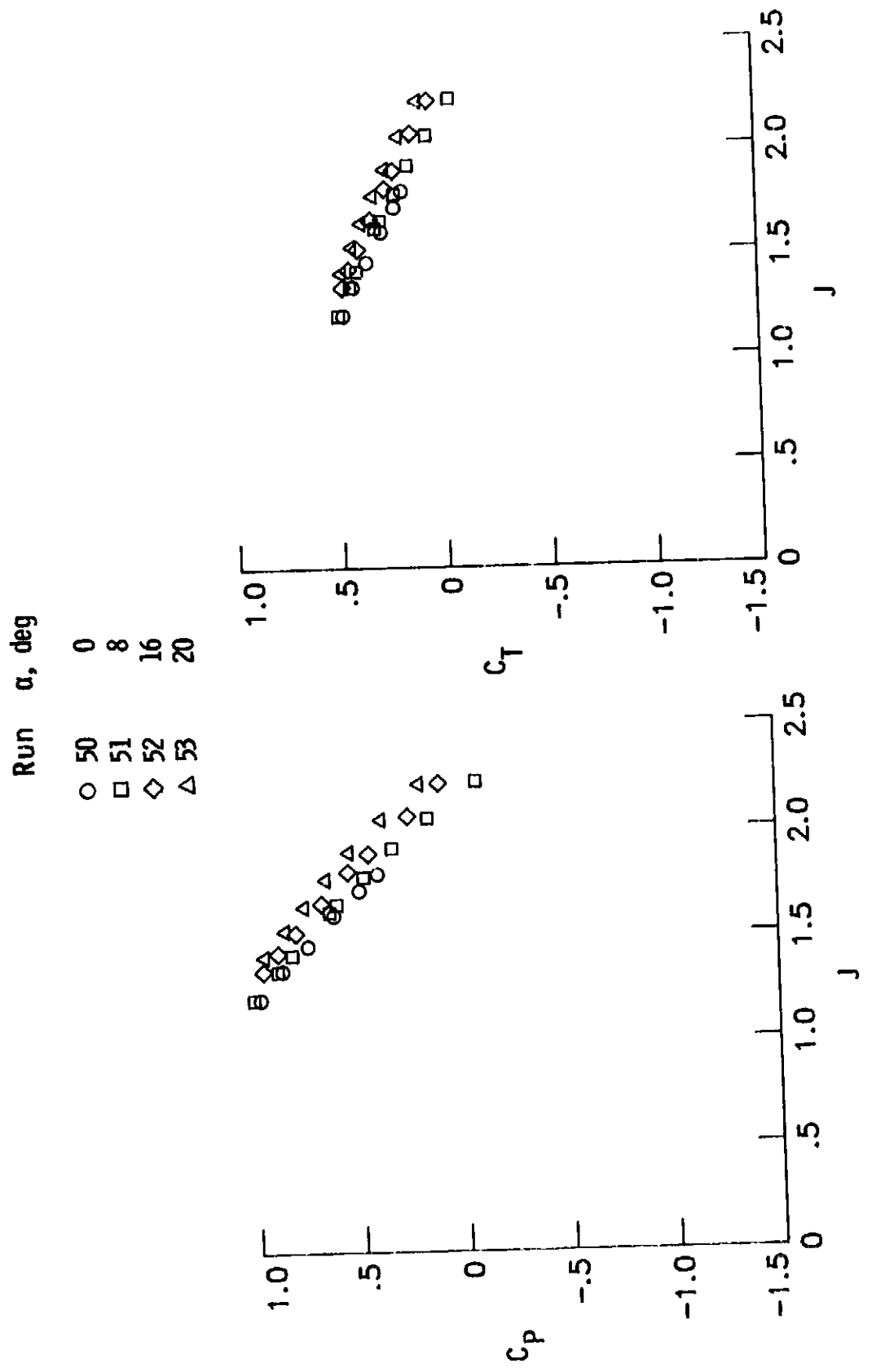
Run α , deg

○	25	0
□	26	4
◊	27	8
△	28	12
▽	29	16
△	30	20



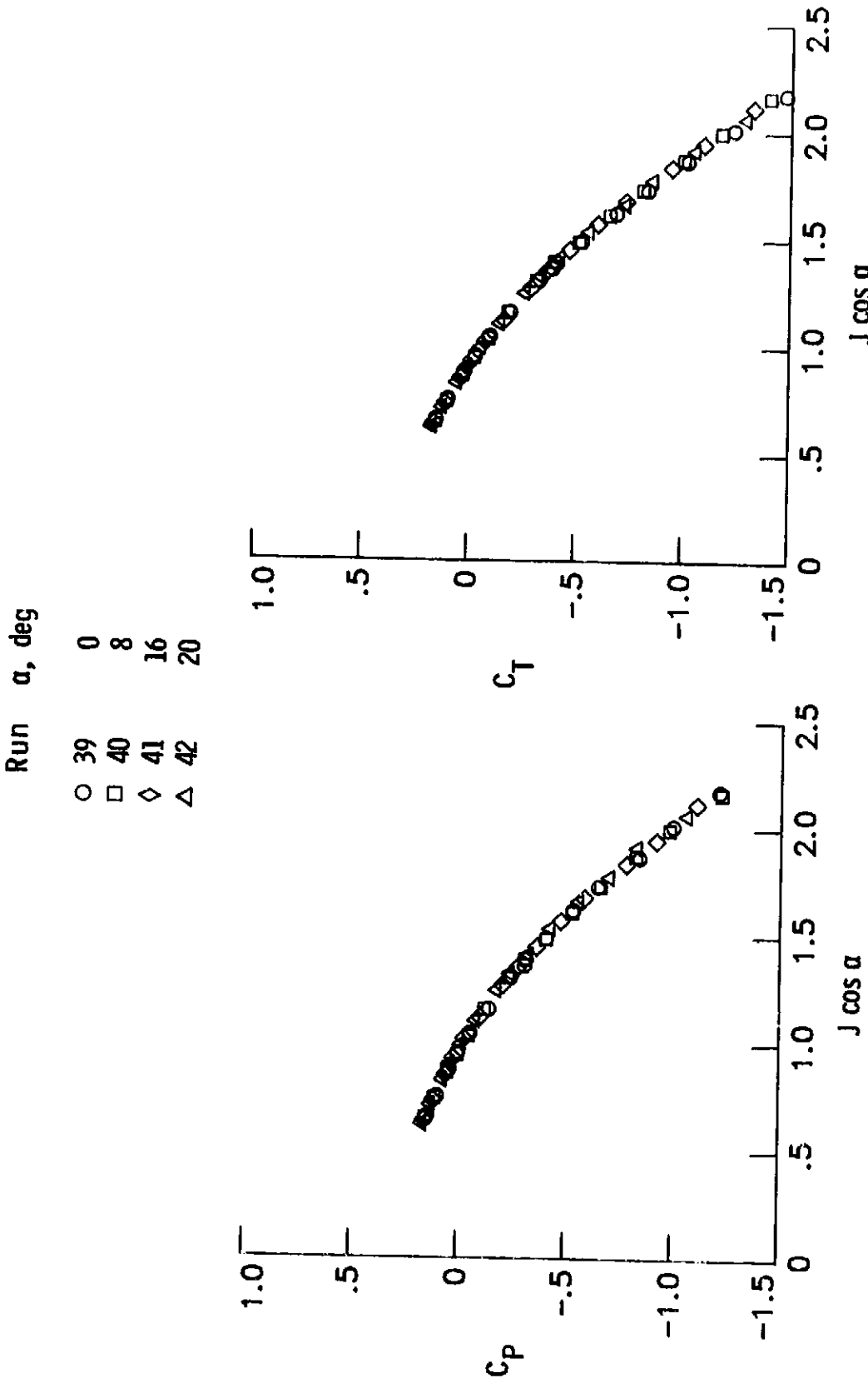
(c) $\beta_{75} = 30.45^\circ$.

Figure 9. Continued.



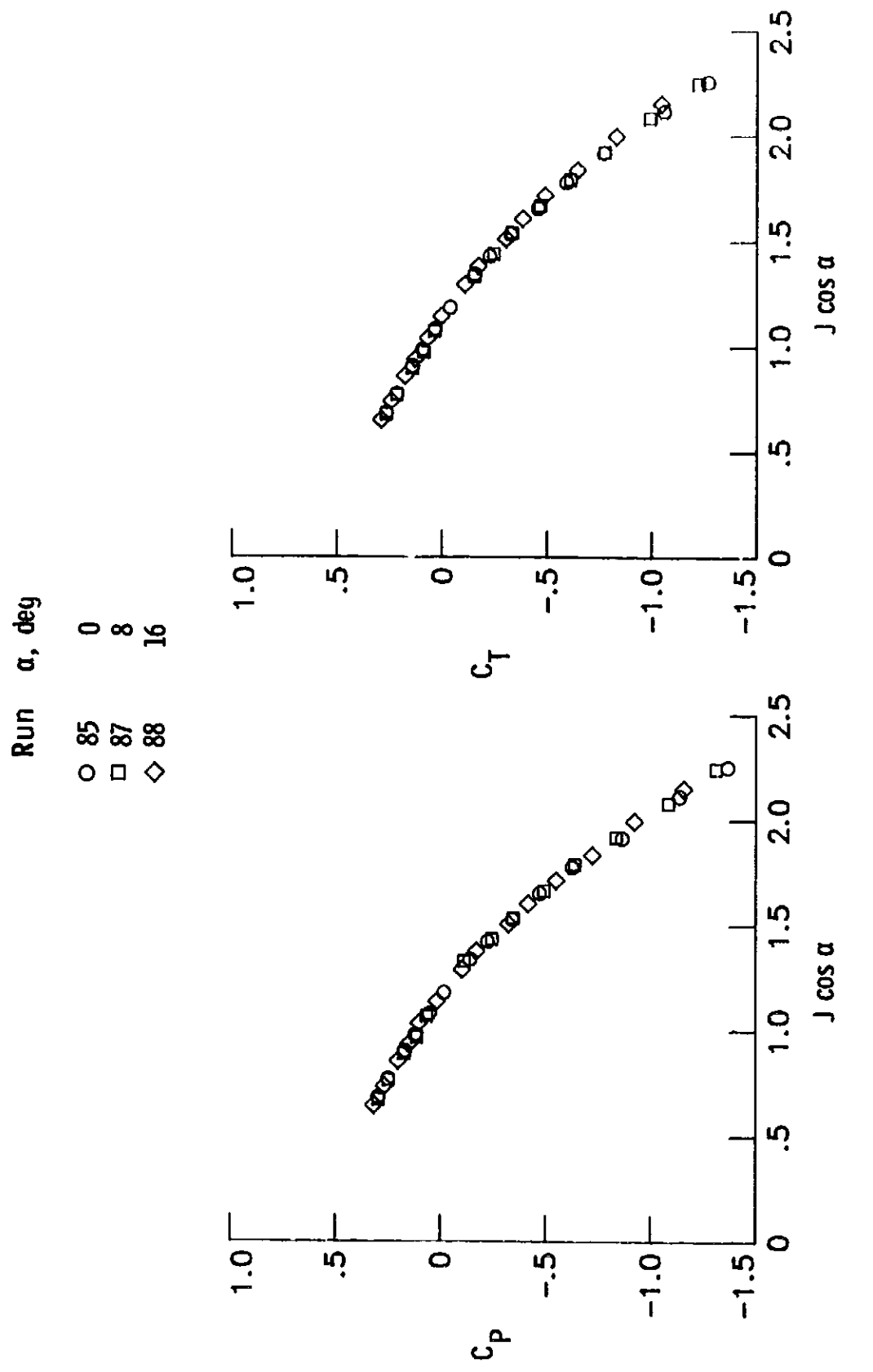
(d) $\beta_{75} = 42.27^\circ$.

Figure 9. Concluded.



(a) $\beta_{75} = 20.59^\circ$.

Figure 10. Propeller performance characteristics plotted against $J \cos \alpha$.



(b) $\beta_{75} = 25.52^\circ$

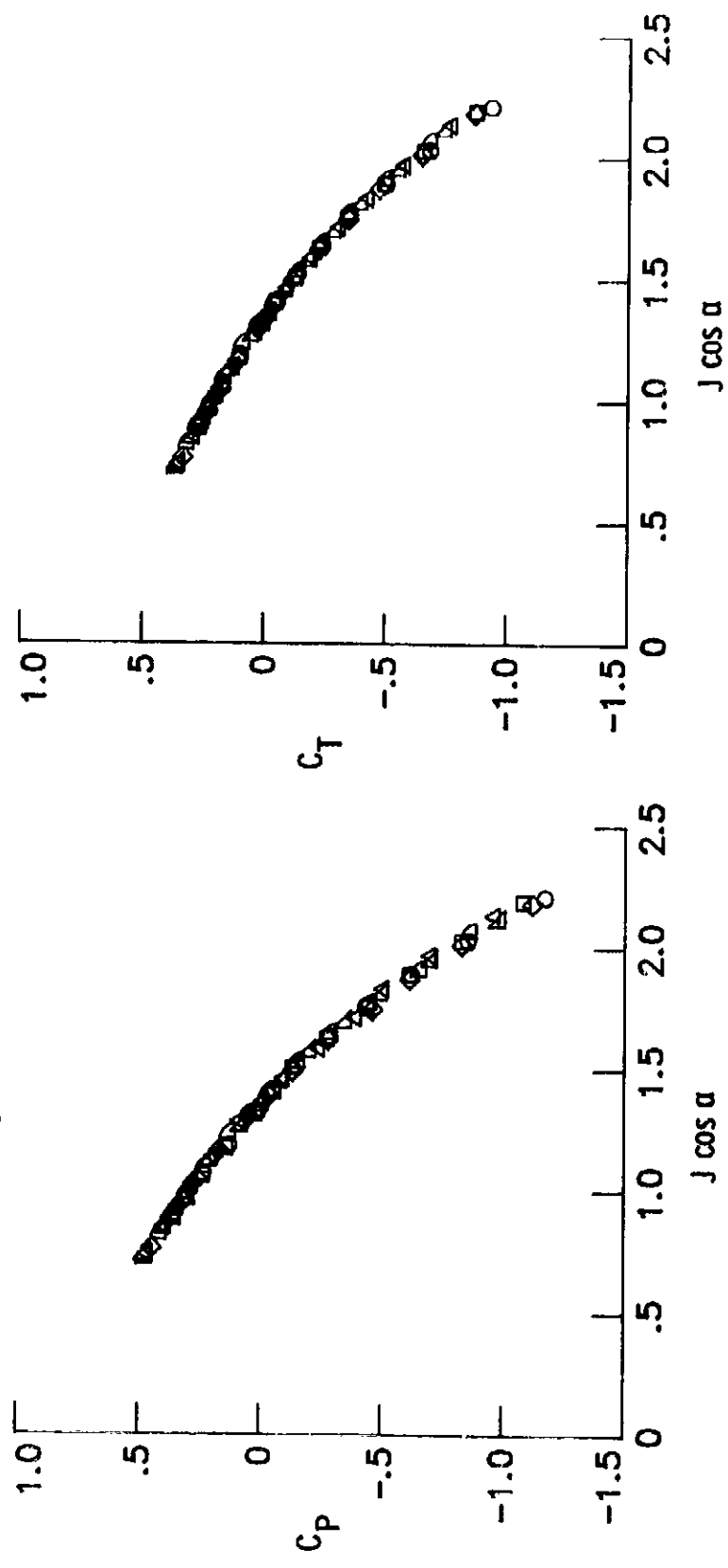
Figure 10. Continued.

Run α , deg

○	25	0
□	26	4
◊	27	8
△	28	12
△	29	16
△	30	20

1.0
.5
0
-.5
-.10
-1.5

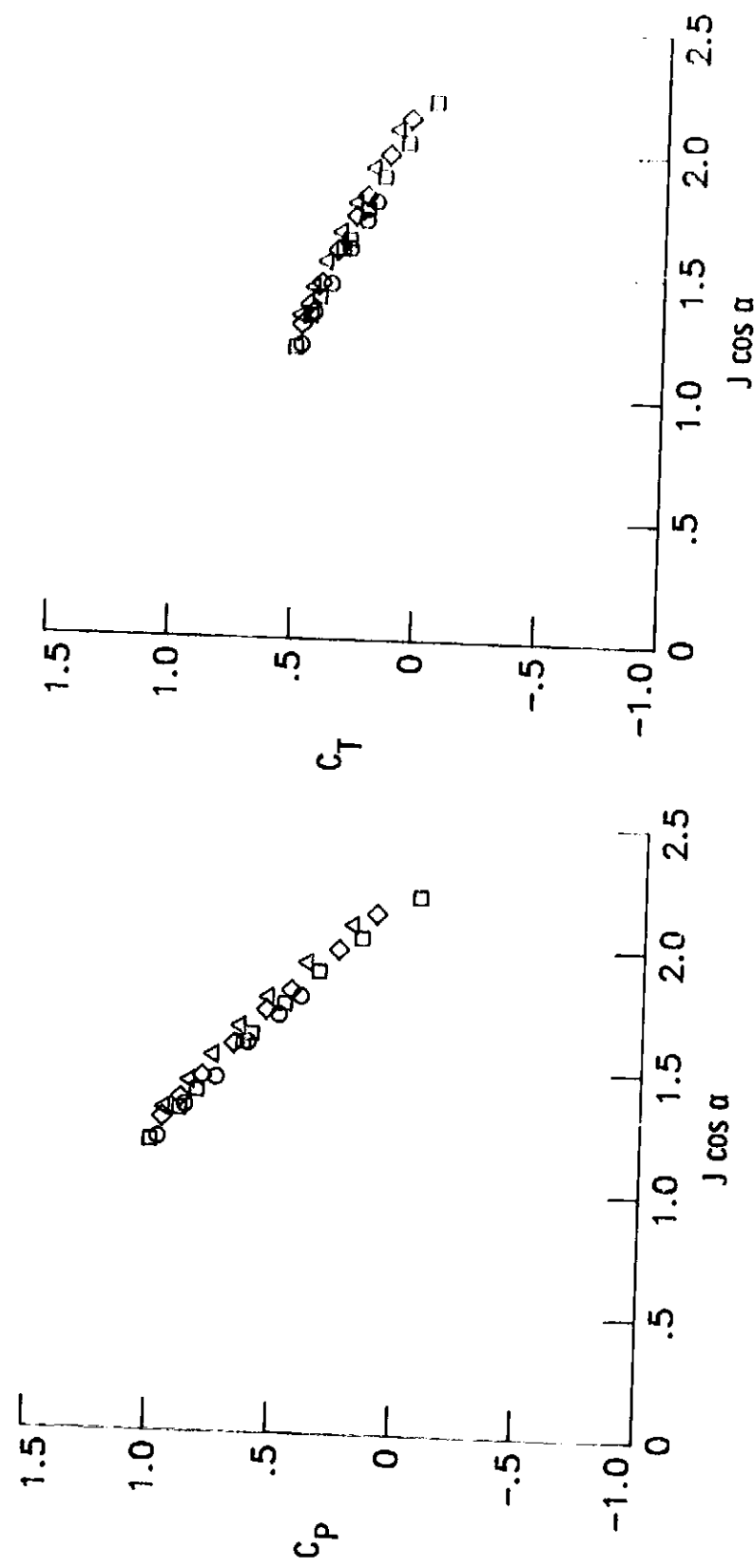
c_T



(c) $\beta_{75} = 30.45^\circ$.

Figure 10. Continued.

Run	α , deg
○ 50	0
□ 51	8
◇ 52	16
△ 53	20



(d) $\beta_{75} = 42.27^\circ$.

Figure 10. Concluded.

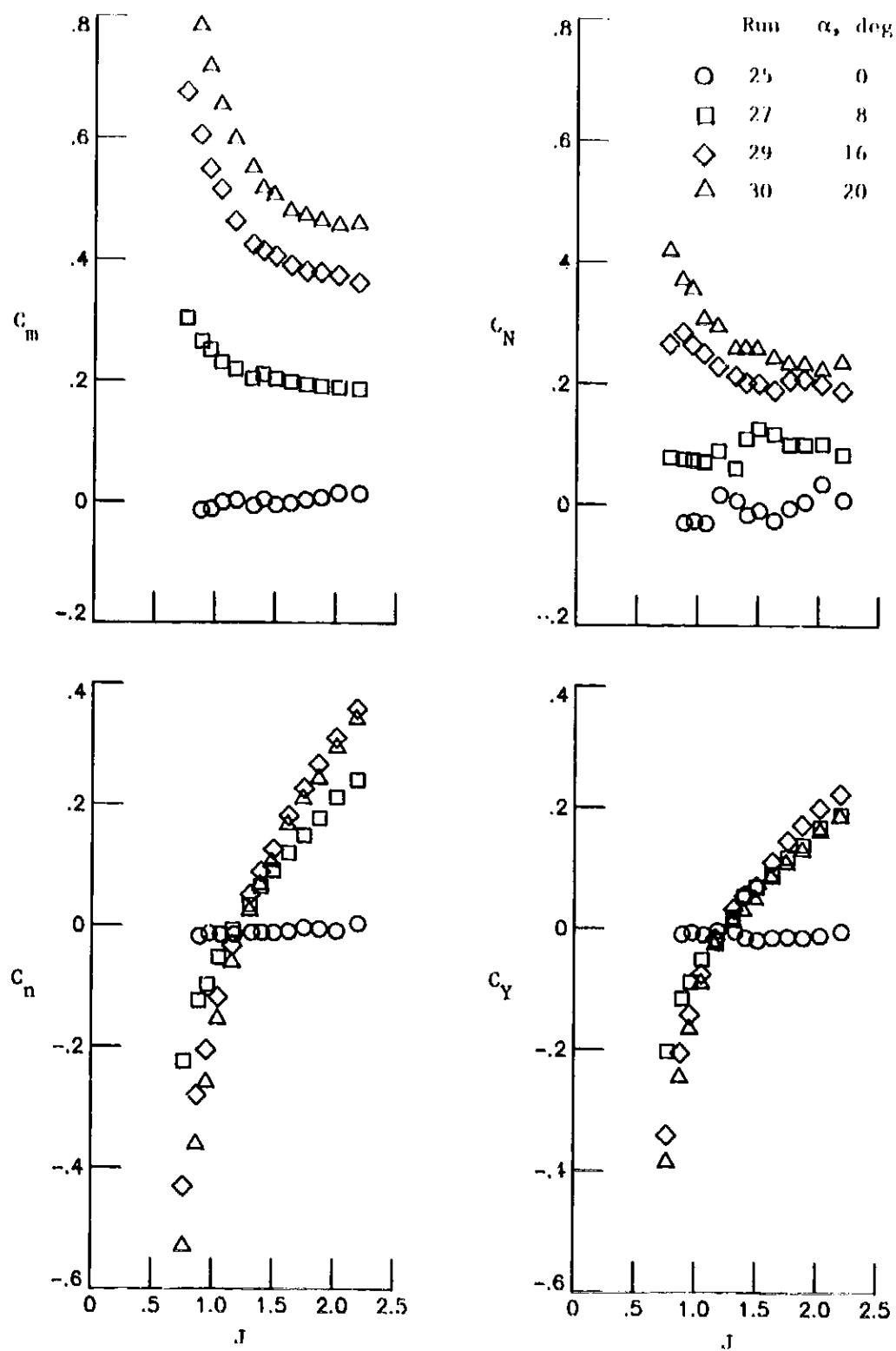


Figure 11. Force and moment characteristics of propeller/nacelle combination. $\beta_{75} = 30.45^\circ$.

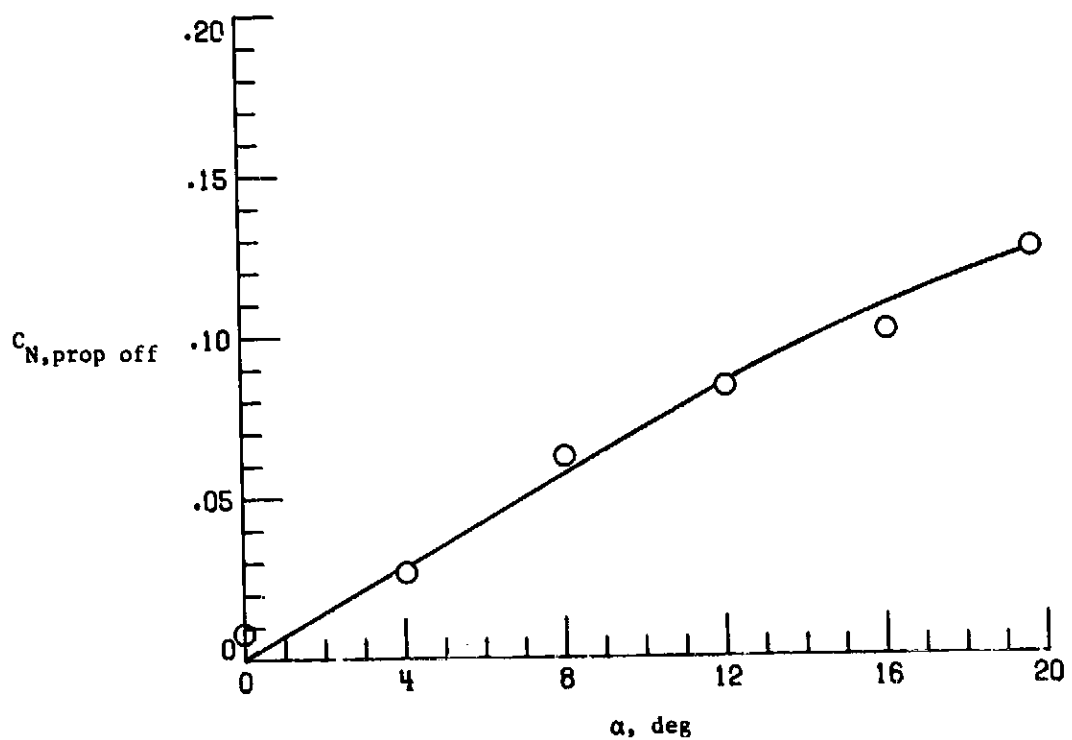
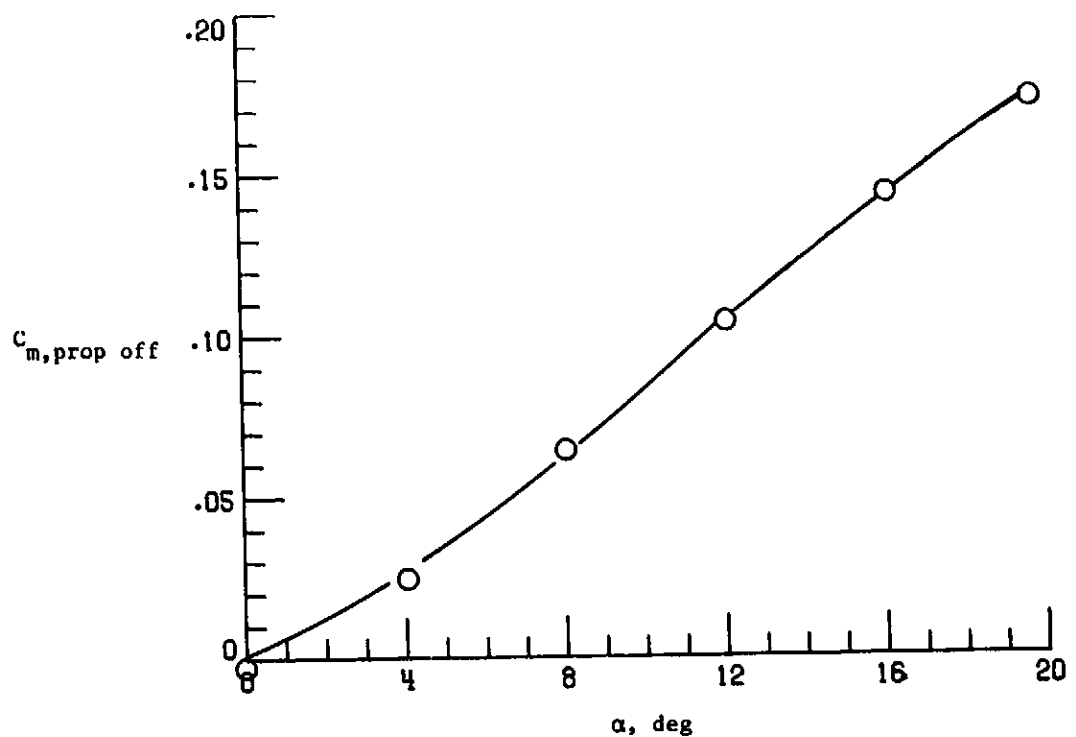


Figure 12. Nacelle pitching-moment and normal-force coefficients plotted against α . Run 31.

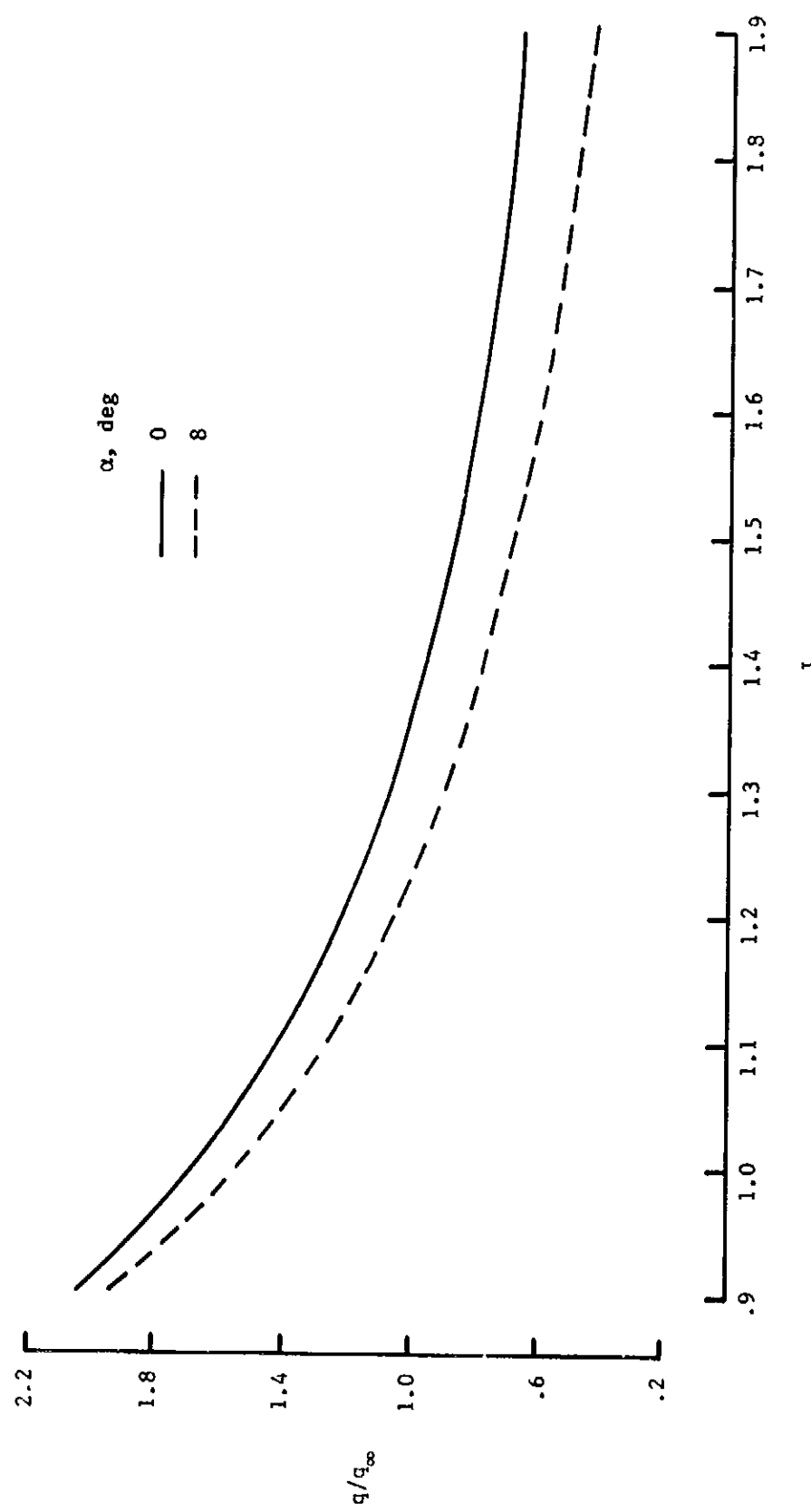


Figure 13. Dynamic pressure ratio measured with pressure probe located 9.0 in. aft of propeller pitch change axis and 5.0 in. from nacelle centerline. $\beta_{.75} = 30.45^\circ$.

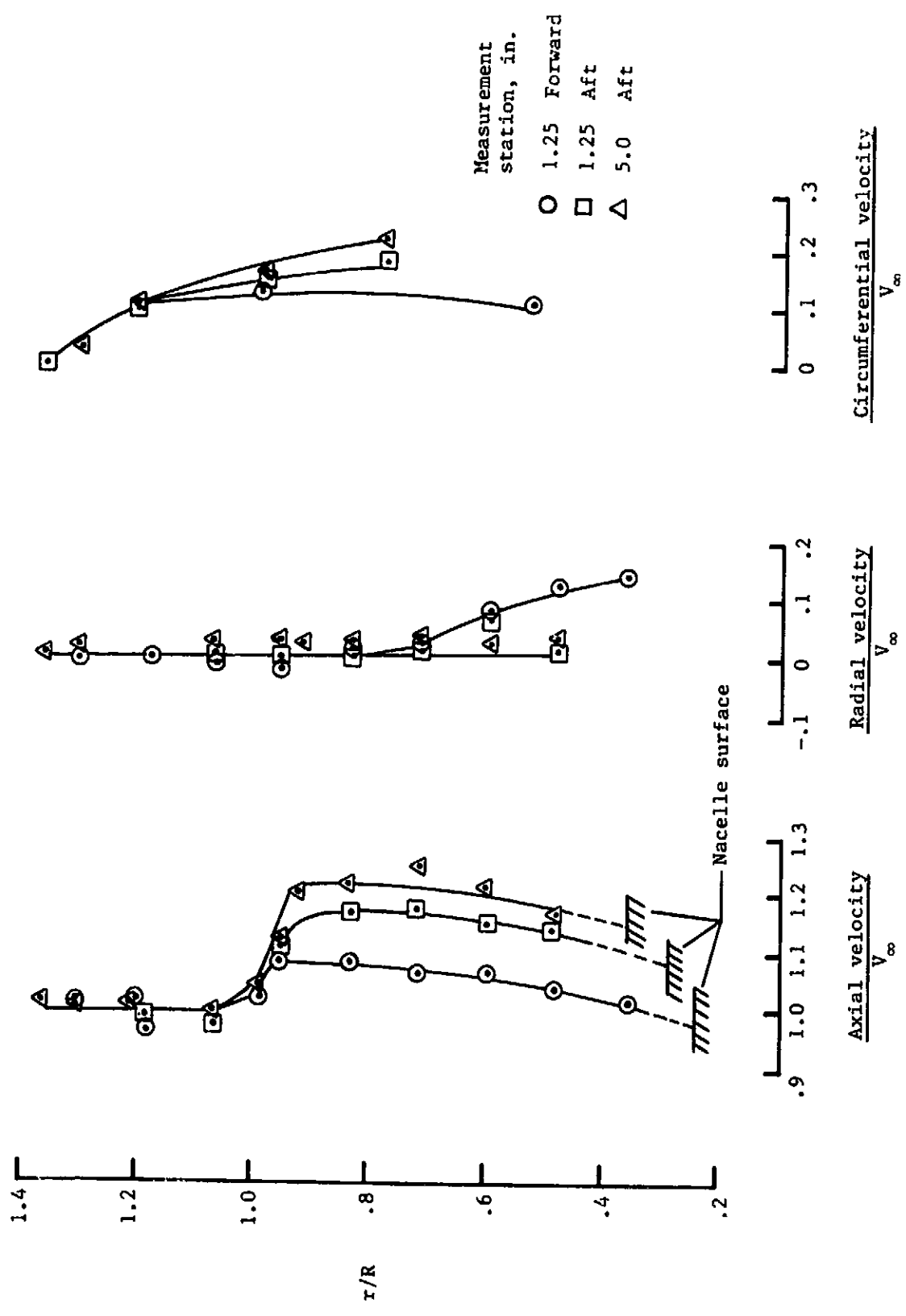


Figure 14. Velocity components as determined from laser velocimeter measurements. Measurement station was relative to propeller pitch change axis. $\beta_{75} = 30.45^\circ$; $J = 1.12$.

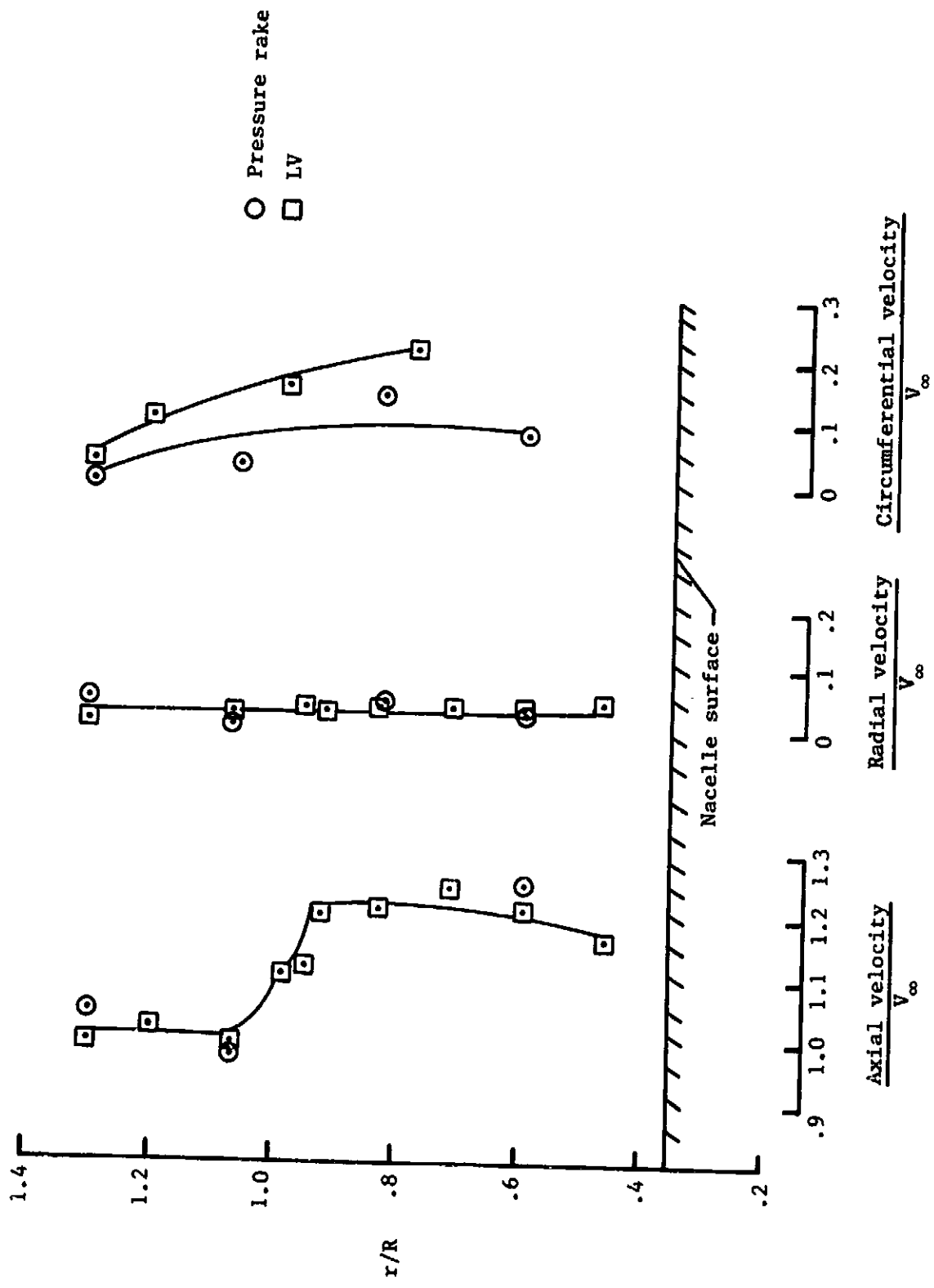


Figure 15. Comparison of velocity ratios based on laser velocimeter (LV) and pressure rake measurements 5.0 in. aft of propeller pitch change axis. $\beta_{.75} = 30.45^\circ; J = 1.1$.

Appendix A

Nondimensional Power Loading

The propeller tested during the present investigation was 1.408 ft in diameter and was driven by a 29-hp (at 10 000 rpm) electric motor. This combination results in a maximum power loading P/d^2 of 14.62 hp/ft². This value of power loading is considerably lower than the values under consideration for full-scale advanced turboprop concepts. However, for conditions wherein compressibility effect can be ignored, such as the low-subsonic flight conditions simulated in these tests, tunnel free-stream velocity can be used as a variable. This permits accurate simulation of propeller performance and flow fields by matching the nondimensional power loading $P/d^2 q_\infty V_\infty$. The derivation of this simulation parameter is given as follows:

Consider the thrust coefficient for an aircraft or wind-tunnel model defined as

$$T_c = T/\rho V_\infty^2 d^2 \quad (A1)$$

Next, consider the standard propeller thrust coefficient defined as

$$C_T = T/\rho n^2 d^4 \quad (A2)$$

Eliminating the thrust term and solving equations (A1) and (A2) for T_c yields

$$T_c = C_T \frac{n^2 d^2}{V_\infty^2} \quad (A3)$$

Next, substituting the advance ratio, $J = V_\infty/nd$, into equation (A3) yields

$$T_c = C_T / J^2 \quad (A4)$$

Therefore, to match aircraft and wind-tunnel-model thrust coefficients T_c , it is necessary to match C_T/J^2 . The advance ratio can be matched for the aircraft and wind-tunnel model by varying the model propeller rotational speed n and the wind-tunnel free-stream velocity V_∞ . It is of course recognized that C_T is affected to some extent by Reynolds number and Mach number, but it is principally a function of propeller blade angle and advance ratio. Therefore, by matching $\beta_{.75}$ and J , C_T will be matched and hence T_c will be matched for the aircraft and wind-tunnel model.

Next, consider the propeller power coefficient defined as

$$C_P = P/\rho n^3 d^5 \quad (A5)$$

and the definition of propeller efficiency given as

$$\eta = J \frac{C_T}{C_P} \quad (A6)$$

By combining equations (A5) and (A6) and the definition of advance ratio, it can be shown that the nondimensional power loading is expressed as

$$\frac{P}{d^2 q_\infty V_\infty} = \frac{2C_T}{J^2 \eta} \quad (A7)$$

From a previous observation that C_T and η are both affected to some extent by Reynolds number and Mach number, but that the principal dependence is on $\beta_{.75}$ and J , it is found that the nondimensional power loading given by equation (A7) is matched between aircraft and wind-tunnel model by matching blade angle and advance ratio.

Appendix B

Propeller Force and Moment Characteristics

Previous propeller analyses (see, for example, ref. 8) have shown that an isolated propeller at angle of attack produces both a normal force and a yawing moment. As noted in the "Results and Discussion" section, the data presented herein include the forces and moments acting on the propeller/nacelle combination that were measured about the balance moment reference center shown in figure 2. The analysis presented in this appendix is an attempt to approximate the normal-force and pitching-moment coefficients of the isolated SR-2 propeller.

Propeller Normal-Force Coefficient

Consider the propeller/nacelle combination acted upon by both the propeller normal force $F_{N,prop}$ and the nacelle normal force $F_{N,nac}$, as depicted in figure B1, in which ξ represents the distance from the point of application of the nacelle normal force to the balance moment reference center. The measured normal force is given by the equation

$$F_{N,meas} = F_{N,prop} + F_{N,nac} \quad (B1)$$

Dividing equation (B1) by $q_\infty S$ yields

$$C_{N,meas} = C_{N,prop} + \frac{F_{N,nac}}{q_\infty S} \quad (B2)$$

With the propeller operating, the nacelle is immersed in the propeller wake and hence operates in a region of dynamic pressure q that differs from q_∞ . Rearranging equation (B2) and introducing q yields

$$C_{N,prop} = C_{N,meas} - \frac{F_{N,nac}}{qS} \frac{q}{q_\infty} \quad (B3)$$

where $C_{N,meas}$ is the quantity C_N presented in figure 11. It should be recognized that

$$\frac{F_{N,nac}}{qS} = C_{N,prop\ off} \quad (B4)$$

which is represented in figure 12 as a function of α . Therefore, the normal-force coefficient of the propeller can be approximated by

$$C_{N,prop} = C_{N,meas} - \frac{q}{q_\infty} C_{N,prop\ off} \quad (B5)$$

where q/q_∞ is presented in figure 13. It should be noted that the dynamic pressure ratio presented in figure 13 is for only one pressure-probe location

(i.e., 9.0 in. aft of the propeller pitch change axis and 5.0 in. from the nacelle centerline) and does not reflect an integrated or average q that the nacelle experiences. Furthermore, these values of q were obtained for only $\alpha = 0^\circ$ and 8° . Recognizing these limitations, approximate values of the propeller normal force have been calculated for $\alpha = 16^\circ$ and 20° by using equation (B5) and data from figures 11, 12, and 13 ($\alpha = 8^\circ$). These results are presented in figure B2.

Propeller Pitching-Moment Coefficient

Again, consider both the propeller/nacelle combination acted upon by the normal forces and the propeller pitching moment $M_{Y,prop}$, as depicted in figure B3. Without the propeller, the symmetric nacelle would produce no pitching moment other than that produced by the normal force acting through the distance ξ . Upon summing the moments about the balance moment reference center, the measured pitching moment $M_{Y,meas}$ is given by

$$M_{Y,meas} = M_{Y,prop} + \ell F_{N,prop} + \xi F_{N,nac} \quad (B6)$$

where ξ can be approximated by

$$\xi = \left. \frac{M_{Y,meas}}{F_{N,nac}} \right|_{prop\ off} \quad (B7)$$

Recognizing that

$$F_{N,prop} = F_{N,meas} - F_{N,nac} \quad (B8)$$

and substituting equations (B8) and (B7) into equation (B6) yields, upon rearranging,

$$\begin{aligned} M_{Y,prop} &= M_{Y,meas} + F_{N,nac} \\ &\times \left(\ell - \left. \frac{M_{Y,meas}}{F_{N,nac}} \right|_{prop\ off} \right) \\ &- \ell F_{N,meas} \end{aligned} \quad (B9)$$

Dividing equation (B9) by $q_\infty S d$ yields

$$\begin{aligned} C_{m,prop} &= C_{m,meas} + \frac{F_{N,nac}}{q_\infty S} \\ &\times \left(\frac{\ell}{d} - \left. \frac{C_{m,meas}}{C_{N,nac}} \right|_{prop\ off} \right) \\ &- \frac{\ell}{d} C_{N,meas} \end{aligned} \quad (B10)$$

As previously noted,

$$\frac{F_{N,nac}}{q_\infty S} \frac{q}{q_\infty} = \frac{q}{q_\infty} (C_{N,nac}|_{\text{prop off}}) \quad (\text{B11})$$

Thus, substituting equation (B11) into (B10) yields

$$\begin{aligned} C_{m,\text{prop}} &= C_{m,\text{meas}} + \frac{q}{q_\infty} (C_{N,nac}|_{\text{prop off}}) \\ &\times \left(\frac{\ell}{d} - \frac{C_{m,\text{meas}}}{C_{N,nac}} \Big|_{\text{prop off}} \right) \\ &- \frac{\ell}{d} C_{N,\text{meas}} \end{aligned} \quad (\text{B12})$$

By substituting the values of C_m and C_N from figure 11, the prop-off values of C_m and C_N from figure 12, and q/q_∞ from figure 13, the propeller pitching-moment coefficient can be approximated and is shown in figure B4.

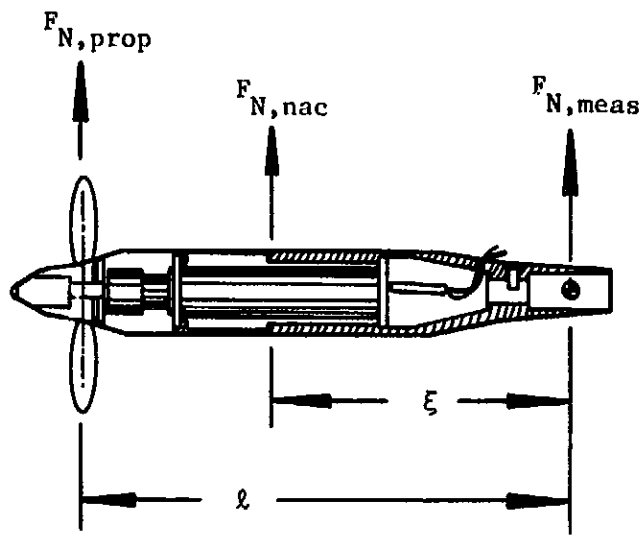


Figure B1. Illustration of normal forces produced by propeller and nacelle.

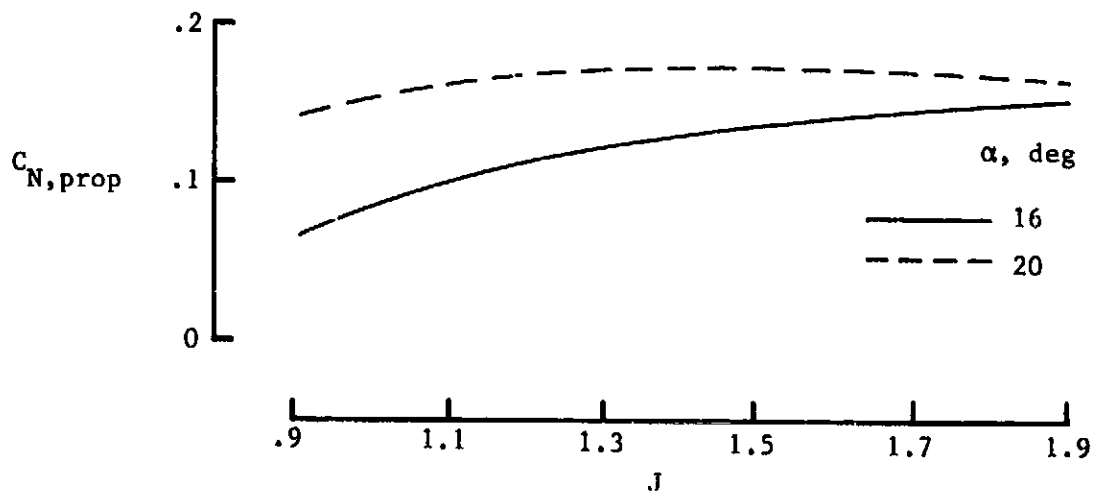


Figure B2. $C_{N,prop}$ plotted against J .

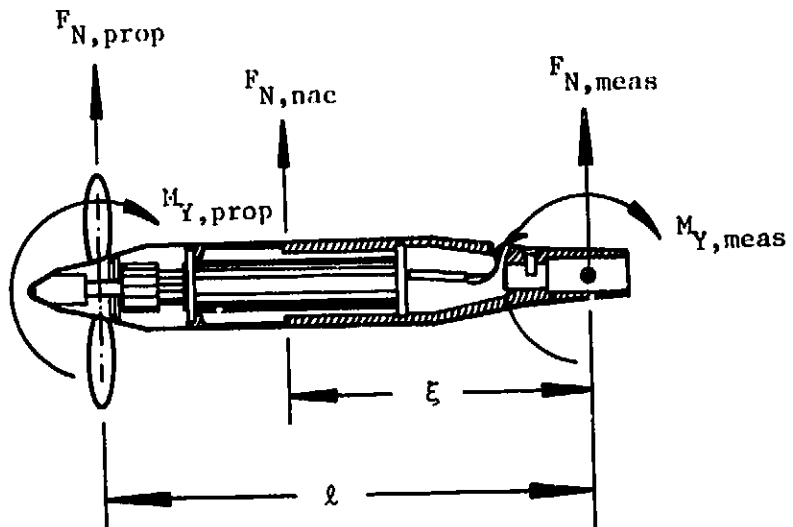


Figure B3. Illustration of normal forces and pitching moment produced by propeller and nacelle.

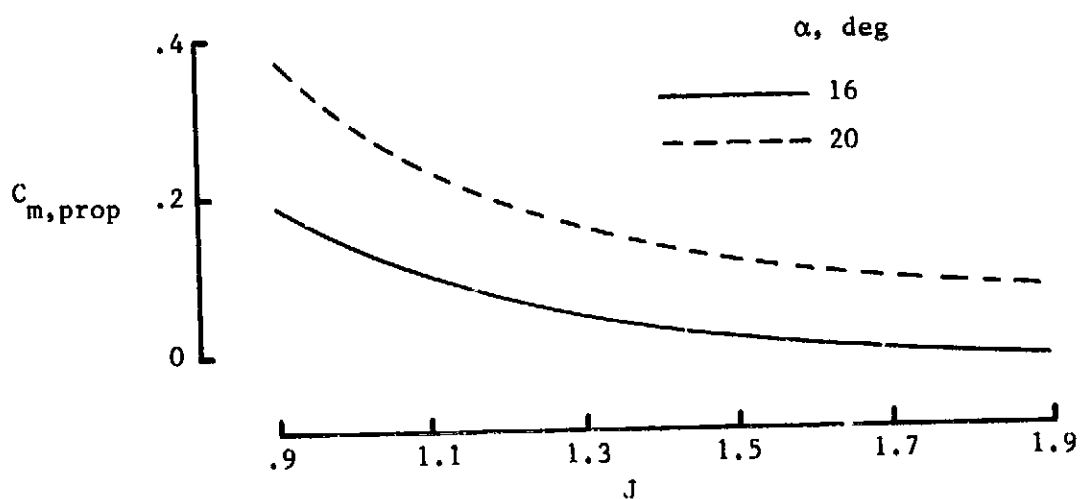


Figure B4. $C_{m,prop}$ plotted against J .

Appendix C

Data Supplement

As an aid to the reader, a run schedule (table CI) and tabular listing of the data (table CII) are presented as follows:

TABLE CI. TEST PROGRAM

Run	β_{75} , deg	α , deg	q , psf	Test section
10	30.45	0	4.5	Open
11		8	4.5	
12		8	18	
13		0	18	
14		0	28	
15		8	28	
16		0	4.5	Closed
17		8	4.5	
18		8	18	
19		0	18	
20		0	28	
21		8	28	
25		0	18	
26		4		
27		8		
28		12		
29		16		
30		20		
31	Blades off 20.59	0 to 20		
39		0		
40		8		
41		16		
42		20		
44	-1.08	0		
50	42.27	0		
51		8		
52		16		
53		20		
85	25.52	0		
87	25.52	8		
88	25.52	16		

TABLE CII. TABULATED DATA

RUN# 10

ALPHA	J	CP	CT	CPM	CNF	CYM	CSF
.06	.4446	.6176	.4791	-.0420	-.1408	-.0871	-.0214
.06	.4906	.5960	.4630	-.0345	-.1618	-.1191	-.0743
.06	.5311	.5738	.4440	-.0074	-.0405	-.1079	-.0799
.08	.5893	.5397	.4200	.0045	-.1362	-.0908	-.0712
.08	.6680	.4937	.3900	.0271	-.1210	-.0579	-.0648
.01	.7081	.4736	.3663	-.0035	-.0907	-.0471	-.0252
.08	.7532	.4470	.3473	.0018	-.1630	-.0740	-.0753
.05	.8229	.3998	.3171	.0130	-.1162	-.0597	-.0669
.05	.8822	.3688	.2918	.0083	-.1510	-.0367	-.0619
.08	.9480	.3259	.2501	.0138	-.1114	-.0383	-.0467
.05	1.0218	.2909	.2106	.0142	-.1098	-.0337	-.0546
.03	1.0977	.2223	.1663	.0252	-.0685	-.0241	-.0178

RUN# 11

ALPHA	J	CP	CT	CPM	CNF	CYM	CSF
8.02	.4515	.6162	.4772	.4678	-.0327	-.7177	-.6536
7.98	.4896	.5943	.4582	.4562	.0104	-.6807	-.6328
8.00	.5373	.5733	.4429	.4069	.0419	-.5888	-.5485
8.00	.5921	.5354	.4168	.3583	-.0660	-.4593	-.4313
8.00	.6707	.4941	.3833	.3400	-.0622	-.3874	-.3600
8.00	.7060	.4772	.3649	.3181	-.0319	-.3455	-.3291
7.98	.7733	.4372	.3374	.2972	-.0290	-.2656	-.2695
8.03	.8184	.4168	.3199	.2975	-.0302	-.2458	-.2486
7.98	.8969	.3601	.2808	.2734	-.0286	-.1817	-.1820
8.00	.9528	.3163	.2508	.2644	-.0669	-.1323	-.1482
7.98	1.0213	.2912	.2151	.2500	-.0688	-.1149	-.1008
8.03	1.1039	.2140	.1793	.2377	-.0706	-.0677	-.0631

RUN# 12

ALPHA	J	CP	CT	CPM	CNF	CYM	CSF
8.00	.8775	.3957	.2915	.2913	.0740	-.1633	-.1383
8.05	.9623	.3385	.2462	.2562	.0581	-.1226	-.0961
8.00	1.0636	.2673	.1910	.2485	.0598	-.0729	-.0631
8.05	1.1670	.1934	.1309	.2368	.0677	-.0372	-.0371
8.05	1.3172	.0716	.0418	.2233	.0578	.0109	.0034
8.00	1.3738	.0219	-.0056	.2122	.0647	.0177	.0045
8.00	1.5136	-.1008	-.0928	.2089	.0660	.0647	.0463
8.02	1.6205	-.2117	-.1792	.2091	.0585	.1018	.0710
8.03	1.7510	-.3401	-.2958	.1962	.0563	.1437	.1057
8.03	1.8972	-.5294	-.4271	.1926	.0568	.1765	.1327
8.00	2.0352	-.7856	-.5897	.1830	.0557	.2006	.1561
8.03	2.1996	-1.0310	-.7787	.2027	.0628	.2505	.1919

TABLE CII. Continued

RUN= 13

ALPHA	J	CP	CT	CPM	CNF	CYM	CSF
.05	.8744	.3805	.2883	-.0021	-.0466	-.0512	-.0303
.01	.9581	.3235	.2423	.0118	-.0304	-.0202	-.0108
.01	1.0552	.2593	.1849	.0239	-.0258	-.0490	-.0344
.05	1.1614	.1874	.1310	.0177	-.0340	-.0106	-.0107
.03	1.3182	.0547	.0296	.0232	-.0224	-.0439	-.0435
.05	1.4149	-.0231	-.0318	.0208	-.0217	-.0265	-.0216
.05	1.5074	-.1193	-.1113	.0055	-.0155	.0086	.0051
.03	1.6219	-.2360	-.2048	.0381	-.0161	-.0487	-.0472
-.01	1.7608	-.4033	-.3287	.0287	-.0183	-.0604	-.0566
.01	1.9024	-.5906	-.4693	.0362	-.0050	-.0038	-.0076
-.01	2.0285	-.7827	-.6296	.0178	-.0187	.0082	-.0008
.03	2.1795	-1.0218	-.8099	.0351	.0057	.0274	.0141

RUN= 14

ALPHA	J	CP	CT	CPM	CNF	CYM	CSF
.01	.8455	.4050	.3057	-.0142	-.0315	-.0314	-.0081
.05	.9577	.3296	.2454	-.0022	-.0301	-.0264	-.0138
.05	1.1047	.2224	.1587	-.0033	-.0161	-.0224	-.0123
.05	1.2001	.1439	.0951	.0094	-.0168	-.0210	-.0144
.05	1.3289	.0414	.0110	.0115	-.0090	-.0150	-.0116
.03	1.4630	-.0903	-.0874	.0075	-.0034	-.0187	-.0162
.01	1.6453	-.2725	-.2389	.0195	-.0043	-.0066	-.0103
.01	1.7774	-.4247	-.3683	.0246	.0034	-.0103	-.0090
.06	1.8875	-.5826	-.4905	.0171	.0018	-.0093	-.0186
.05	2.0442	-.8154	-.6803	.0213	.0092	-.0151	-.0192
.01	2.2273	-1.1299	-.9439	.0414	.0102	-.0018	-.0106
.03	2.3421	-1.3488	-1.1093	.0400	.0213	-.0136	-.0156
.05	2.5657	-1.7443	-1.4532	.0232	.0052	-.0119	-.0182
.03	2.7350	-2.0574	-1.7168	.0437	.0233	.0004	-.0073

RUN= 15

ALPHA	J	CP	CT	CPM	CNF	CYM	CSF
8.00	.8378	.4185	.3067	.2961	.0897	-.1765	-.1495
8.02	.9517	.3403	.2475	.2677	.0870	-.1150	-.0935
7.96	1.0994	.2365	.1605	.2304	.0815	-.0455	-.0316
8.00	1.2077	.1502	.0959	.2250	.0827	.0042	-.0013
8.02	1.3230	.0583	.0234	.2138	.0817	.0349	.0267
8.02	1.4563	-.0683	-.0654	.2051	.0753	.0671	.0525
8.03	1.6552	-.2725	-.2284	.1998	.0703	.1123	.0871
7.96	1.7854	-.4150	-.3421	.2015	.0841	.1416	.1136
7.98	1.8922	-.5628	-.4612	.1925	.0655	.1759	.1363
8.00	2.0499	-.8008	-.6427	.2036	.0814	.1986	.1572
8.00	2.2318	-1.0967	-.8566	.1957	.0751	.2433	.1932
7.98	2.3932	-1.4045	-1.0944	.1837	.0729	.2735	.2168
8.03	2.5693	-1.7004	-1.3225	.1977	.0832	.2970	.2324
7.96	2.7617	-2.0366	-1.6086	.2027	.0974	.3123	.2542

TABLE CH. Continued

RUN# 16

ALPHA	J	CP	CT	CPM	CNF	CYM	CSF
.06	.4412	.6069	.4754	-.0350	-.1694	.0125	.0420
.05	.4794	.5834	.4600	-.0345	-.1993	-.0439	.0023
.05	.5259	.5596	.4411	-.0066	-.1460	-.0327	-.0002
.03	.5839	.5375	.4177	-.0418	-.1494	-.0274	-.0049
.05	.6574	.4959	.3863	-.0357	-.1759	-.0534	-.0436
.03	.6839	.4771	.3707	-.0359	-.2139	-.0357	-.0267
.03	.7394	.4482	.3499	-.0193	-.2057	-.0377	-.0533
.01	.8130	.4054	.3143	-.0284	-.1635	-.0159	-.0226
.05	.8806	.3662	.2847	.0032	-.1523	-.0237	-.0842
.01	.9278	.3306	.2501	-.0070	-.1940	-.0176	-.0361
.01	.9971	.2927	.2164	-.0121	-.1940	-.0179	-.0441
.06	1.0915	.1905	.1715	-.0170	-.1926	-.0008	-.0502

RUN# 17

ALPHA	J	CP	CT	CPM	CNF	CYM	CSF
8.02	.4375	.6122	.4745	.4898	.0038	-.7307	-.6631
7.96	.4840	.5874	.4552	.4424	.0433	-.6127	-.5797
8.02	.5303	.5548	.4383	.4272	.0494	-.5218	-.4935
8.00	.5894	.5243	.4134	.3587	-.0298	-.4334	-.4091
7.96	.6561	.4940	.3845	.3140	.0363	-.3549	-.3373
7.98	.6823	.4650	.3672	.3112	.0004	-.3411	-.3156
8.03	.7409	.4390	.3465	.2830	-.0041	-.2795	-.2848
8.02	.8008	.4124	.3168	.2686	-.0407	-.2370	-.2210
7.98	.8738	.3615	.2793	.2392	-.0437	-.1791	-.1684
8.02	.9227	.3247	.2578	.2328	-.0072	-.1460	-.1536
8.00	1.0000	.2701	.2202	.2395	-.0758	-.1126	-.1145
8.02	1.0744	.2276	.1827	.2286	-.0402	-.0780	-.0887

RUN# 18

ALPHA	J	CP	CT	CPM	CNF	CYM	CSF
8.03	.8828	.3750	.2798	.2700	.0768	-.1566	-.1321
8.02	.9653	.3216	.2959	.2533	.0584	-.1081	-.0910
8.00	1.0561	.2663	.1866	.2445	.0590	-.0612	-.0545
7.98	1.1592	.1812	.1252	.2378	.0510	-.0212	-.0171
7.98	1.3120	.0599	.0300	.2099	.0641	.0299	.0232
8.02	1.3740	.0174	-.0109	.1978	.0521	.0434	.0328
8.03	1.4944	-.1145	-.0951	.1955	.0623	.0759	.0548
8.03	1.5922	-.2173	-.1739	.1904	.0712	.0992	.0762
8.00	1.7724	-.3982	-.3244	.1877	.0634	.1418	.1078
8.00	1.8825	-.5691	-.4389	.1814	.0537	.1594	.1260
8.03	2.0068	-.7283	-.5763	.1736	.0525	.1948	.1520
7.98	2.2229	-1.1112	-.8556	.1823	.0660	.2258	.1827

TABLE CH. Continued

RUN# 19

ALPHA	J	CP	CT	CPM	CNF	CYM	CSF
.05	.8816	.3654	.2773	-.0028	-.0004	-.0084	.0006
.06	.9101	.3336	.2584	.0012	-.0160	-.0171	.0010
.05	.9572	.3197	.2379	.0013	-.0151	-.0207	-.0025
.05	1.0532	.2495	.1821	-.0008	-.0134	-.0103	-.0032
.10	1.1561	.1582	.1220	.0061	-.0006	-.0137	-.0018
.05	1.3140	.0279	.0173	.0076	-.0076	-.0194	-.0089
.05	1.3855	-.0275	-.0308	.0053	-.0073	-.0014	.0006
.10	1.4982	-.1138	-.1112	.0066	.0025	-.0111	-.0037
.10	1.6052	-.2572	-.2013	.0068	.0036	-.0063	-.0045
.08	1.7913	-.4568	-.3730	.0042	-.0056	-.0105	-.0167
.06	1.8677	-.5877	-.4631	.0174	-.0011	-.0044	-.0045
.10	2.0241	-.8141	-.6436	.0189	-.0003	-.0073	-.0062
.05	2.1485	-1.0222	-.8232	.0176	.0086	-.0131	-.0139

RUN# 20

ALPHA	J	CP	CT	CPM	CNF	CYM	CSF
.06	.8314	.4075	.3098	-.0027	-.0056	-.0108	.0048
.05	.9371	.3332	.2505	.0054	.0003	-.0196	-.0024
.03	1.0904	.2202	.1547	-.0033	-.0046	-.0164	-.0054
.10	1.1862	.1469	.0996	.0097	.0065	-.0127	-.0078
.08	1.3089	.0430	.0176	.0099	.0080	-.0120	-.0065
.05	1.4252	-.0592	-.0697	.0067	.0079	-.0134	-.0061
.08	1.6393	-.2859	-.2440	.0160	.0119	-.0153	-.0084
.08	1.7507	-.4044	-.3425	.0145	.0121	-.0077	-.0057
.10	1.8662	-.5620	-.4736	.0170	.0074	-.0142	-.0115
.10	2.0298	-.8231	-.6799	.0179	.0141	-.0125	-.0100
.06	2.1875	-1.0653	-.8841	.0298	.0181	-.0073	-.0110
.10	2.3503	-1.3613	-1.1424	.0272	.0234	-.0074	-.0100
.08	2.5133	-1.6797	-1.3987	.0245	.0234	.0027	.0012
.05	2.7214	-2.0725	-1.7322	.0266	.0297	-.0017	-.0035

RUN# 21

ALPHA	J	CP	CT	CPM	CNF	CYM	CSF
7.98	.8327	.4190	.3085	.2988	.1017	-.1777	-.1434
7.98	.9347	.3437	.2535	.2693	.0935	-.1083	-.0842
7.98	1.0857	.2356	.1673	.2339	.0887	-.0331	-.0248
7.98	1.1901	.1575	.1053	.2296	.0901	.0041	.0056
7.96	1.3060	.0577	.0269	.2159	.0942	.0335	.0321
7.98	1.4357	-.0554	-.0634	.2062	.0815	.0675	.0358
7.92	1.6243	-.2523	-.2129	.2030	.0891	.1126	.0910
7.90	1.7241	-.3724	-.3063	.1908	.0811	.1367	.1125
7.94	1.8920	-.5839	-.4727	.1818	.0742	.1757	.1424
7.96	2.0683	-.8578	-.6692	.1835	.0760	.2099	.1682
7.92	2.2152	-1.0865	-.8564	.1849	.0836	.2441	.1963
7.96	2.3462	-1.3375	-1.0577	.1872	.0852	.2630	.2122
7.92	2.5121	-1.6473	-.2951	.1909	.0932	.2827	.2324
7.96	2.7365	-2.0377	-.5974	.1905	.0878	.3081	.2577

TABLE CII. Continued

RUN = 25

ALPHA	J	CP	CT	CPM	CNF	CYM	CSF
.07	.8897	.3609	.2757	-.0144	-.0302	-.0181	-.0095
.05	.9733	.3027	.2283	-.0126	-.0272	-.0140	-.0069
.01	1.0683	.2320	.1717	-.0008	-.0307	-.0155	-.0104
.03	1.1844	.1260	.1011	.0022	.0164	-.0154	-.0037
.05	1.3266	.0050	.0056	-.0066	.0066	-.0121	-.0057
.05	1.4126	-.0511	-.0544	.0038	-.0167	-.0122	-.0155
.03	1.5122	-.1531	-.1337	-.0052	-.0097	-.0123	-.0195
.05	1.6341	-.2856	-.2379	-.0025	-.0262	-.0102	-.0151
.07	1.7606	-.4376	-.3496	.0030	-.0058	-.0039	-.0139
.01	1.8881	-.6240	-.5010	.0070	.0049	-.0059	-.0155
.03	2.0294	-.8585	-.6806	.0151	.0349	-.0091	-.0118
.01	2.2077	-1.1728	-.9351	.0138	.0083	.0032	-.0046

RUN = 26

ALPHA	J	CP	CT	CPM	CNF	CYM	CSF
3.96	.8886	.3534	.2714	.1176	.0625	-.0774	-.0338
3.98	.9700	.2955	.2256	.1118	.0550	-.0485	-.0348
3.98	1.0642	.2337	.1731	.1058	.0202	-.0313	-.0275
3.92	1.1778	.1379	.1030	.1159	.0706	-.0049	.0010
3.92	1.3194	.0172	.0071	.1080	.0617	.0189	.0158
3.98	1.4091	-.0576	-.0462	.1066	.0802	.0317	.0228
3.92	1.5084	-.1349	-.1267	.0966	.0333	.0456	.0328
3.98	1.6305	-.2788	-.2241	.0992	.0261	.0602	.0403
3.95	1.7559	-.4419	-.3414	.1015	.0279	.0759	.0561
3.96	1.8942	-.6162	-.4927	.0783	.0218	.0811	.0566
3.92	2.0303	-.8320	-.6558	.0899	.0269	.1191	.0889
3.92	2.1950	-1.0830	-.8706	.0971	.0204	.1206	.0988

RUN = 27

ALPHA	J	CP	CT	CPM	CNF	CYM	CSF
8.00	.7711	.4436	.3338	.3023	.0774	-.2252	-.2034
7.94	.8933	.3654	.2705	.2642	.0745	-.1248	-.1163
8.00	.9643	.3142	.2312	.2501	.0730	-.0987	-.0891
8.00	1.0565	.2555	.1789	.2302	.0704	-.0535	-.0517
7.94	1.1728	.1675	.1093	.2186	.0887	-.0083	-.0198
7.96	1.3136	.0464	.0198	.2032	.0598	.0331	.0181
8.00	1.4034	-.0380	-.0393	.2099	.1088	.0636	.0534
8.00	1.5060	-.1364	-.1157	.2025	.1255	.0903	.0682
8.00	1.6352	-.2829	-.2243	.1977	.1167	.1195	.0896
7.96	1.7620	-.4635	-.3459	.1933	.0091	.1483	.1167
8.00	1.8897	-.6191	-.4734	.1906	.0994	.1760	.1373
7.96	2.0313	-.8342	-.6486	.1888	.1006	.2114	.1664
8.00	2.2023	-1.1230	-.8661	.1861	.0828	.2400	.1873

TABLE CHI. Continued

RUN= 28

ALPHA	J	CP	CT	CPM	CNF	CYM	CSF
11.94	.7555	.4601	.3463	.5093	.1895	-.3523	-.2950
11.96	.8725	.3910	.2860	.4191	.1451	-.2170	-.1785
11.98	.9569	.3331	.2426	.3907	.1591	-.1514	-.1266
11.98	1.0518	.2722	.1911	.3721	.1391	-.0843	-.0761
11.96	1.1652	.1809	.1236	.3334	.1227	-.0208	-.0269
11.98	1.3145	.0796	.0320	.3262	.1515	.0524	.0360
11.96	1.3967	-.0166	-.0263	.3037	.1563	.0802	.0554
11.94	1.4952	-.1013	-.0936	.3004	.1479	.1119	.0769
11.96	1.6220	-.2476	-.1947	.2855	.1450	.1512	.1095
11.94	1.7514	-.3976	-.3091	.2837	.1465	.1979	.1393
11.94	1.8721	-.5104	-.4242	.2765	.1003	.2384	.1612
11.92	2.0123	-.7050	-.5764	.2706	.1093	.2704	.1822
11.96	2.1821	-.9670	-.7688	.2649	.1180	.3166	.2219

RUN= 29

ALPHA	J	CP	CT	CPM	CNF	CYM	CSF
15.98	.7651	.4692	.3516	.6750	.2651	-.4318	-.3416
15.94	.8776	.3879	.2944	.6046	.2841	-.2810	-.2061
15.94	.9559	.3416	.2549	.5487	.2639	-.2064	-.1426
15.94	1.0504	.2812	.2048	.5155	.2495	-.1191	-.0756
15.98	1.1677	.2015	.1430	.4628	.2287	-.0340	-.0174
15.96	1.3164	.0727	.0465	.4245	.2122	.0506	.0320
15.98	1.4033	.0019	-.0102	.4141	.2016	.0882	.0534
15.98	1.5065	-.0885	-.0820	.4054	.2002	.1253	.0687
15.98	1.6360	-.2077	-.1794	.3904	.1890	.1809	.1095
15.98	1.7627	-.3554	-.2905	.3805	.2061	.2259	.1444
15.96	1.8802	-.5023	-.3987	.3788	.2074	.2662	.1706
15.94	2.0257	-.7100	-.5550	.3742	.1995	.3098	.1984
15.98	2.1969	-.9876	-.7459	.3621	.1R82	.3578	.2223

RUN= 30

ALPHA	J	CP	CT	CPM	CNF	CYM	CSF
19.98	.7705	.4708	.3617	.8881	.4187	-.5315	-.3861
20.00	.8760	.4086	.3151	.7830	.3700	-.3629	-.2466
20.00	.9578	.3595	.2755	.7163	.3548	-.2608	-.1665
19.94	1.0524	.3014	.2240	.6534	.3062	-.1560	-.0911
19.96	1.1677	.2256	.1648	.5975	.2939	-.0624	-.0278
19.98	1.3147	.1251	.0879	.5502	.2571	.0229	.0101
19.96	1.4001	.0435	.0269	.5162	.2579	.0658	.0289
19.98	1.4942	-.0369	-.0380	.5048	.2566	.1035	.0476
19.98	1.6309	-.1587	-.1398	.4787	.2417	.1651	.0829
19.98	1.7539	-.2935	-.2363	.4710	.2316	.2082	.1063
19.96	1.8853	-.4536	-.3473	.4628	.2310	.2417	.1272
19.96	2.0320	-.6594	-.5015	.4555	.2218	.2931	.1594
19.92	2.1968	-.8672	-.6810	.4586	.2345	.3402	.1836

TABLE CII. Continued

RUN# 31

ALPHA	J	CP	CT	CPM	CNF	CYM	CSF
-8.03	-----	-----	-----	-.0522	-.0067	-.0016	-.0001
-3.96	-----	-----	-----	-.0196	.0056	-.0063	-.0029
-.01	-----	-----	-----	-.0026	.0082	-.0052	-.0027
4.05	-----	-----	-----	.0248	.0268	-.0078	.0000
8.04	-----	-----	-----	.0644	.0624	-.0044	.0052
12.05	-----	-----	-----	.1040	.0839	-.0092	.0046
16.09	-----	-----	-----	.1434	.1008	-.0077	-.0045
19.70	-----	-----	-----	.1726	.1260	-.0106	-.0055

RUN# 39

ALPHA	J	CP	CT	CPM	CNF	CYM	CSF
-.03	.6587	.1418	.1465	.0014	-.0152	-.0333	-.0156
-.09	.7527	.0947	.0915	.0019	-.0212	-.0288	-.0148
-.09	.8781	.0377	.0191	.0049	-.0360	-.0114	-.0100
-.05	.9550	-.0005	-.0336	.0104	-.0155	-.0120	-.0140
-.07	1.0469	-.0569	-.1020	.0133	-.0230	-.0092	-.0063
-.05	1.1600	-.1434	-.1962	.0042	-.0157	-.0097	-.0071
-.09	1.3117	-.2472	-.3316	.0280	.0011	-.0165	-.0170
-.05	1.3639	-.3090	-.3908	.0230	-.0181	-.0054	-.0075
-.10	1.3895	-.3111	-.4093	.0232	.0003	-.0001	-.0051
-.09	1.4909	-.4078	-.5256	.0234	-.0081	.0136	.0016
-.09	1.6219	-.5342	-.6865	.0273	-.0060	.0278	.0166
-.07	1.7310	-.6475	-.8326	.0315	-.0152	-.0102	-.0057
-.09	1.8679	-.8404	-1.0187	.0166	.0091	.0016	.0009
-.10	2.0139	-.9969	-1.2334	.0328	.0150	.0404	.0391
-.12	2.1769	-1.2122	-1.4747	.0276	.0041	.0267	.0215

RUN# 40

ALPHA	J	CP	CT	CPM	CNF	CYM	CSF
8.01	.6565	.1498	.1482	.2237	.0607	-.1657	-.1390
8.03	.7516	.1067	.0970	.2022	.0410	-.0856	-.0731
8.03	.8739	.0483	.0241	.1793	.0479	-.0057	-.0060
7.99	.9566	.0004	-.0302	.1658	.0463	.0304	.0220
7.99	1.0448	-.0515	-.0953	.1551	.0545	.0746	.0557
7.99	1.1689	-.1232	-.1847	.1562	.0562	.1019	.0737
7.99	1.3184	.2353	-.3152	.1302	.0414	.1407	.1068
7.97	1.4075	-.3098	-.3984	.1181	.0302	.1733	.1324
7.97	1.5021	-.4100	-.5131	.1232	.0421	.2074	.1568
7.97	1.6277	-.5295	-.6555	.0931	.0253	.2362	.1832
7.97	1.7496	-.6601	-.8109	.1105	.0313	.2583	.1951
7.99	1.8923	-.8252	-1.0002	.0995	.0111	.2905	.2229
8.03	2.0173	-.9802	-1.1796	.1006	.0391	.3136	.2315
8.03	2.1860	-1.2223	-1.4020	.1109	.0433	.3480	.2590

TABLE CH. Continued

RUN# 41

ALPHA	J	CP	CT	CPM	CNF	CYM	CSF
15.92	.6647	.1547	.1575	.4855	.1850	-.2941	-.2110
15.97	.7611	.1126	.1052	.4094	.1596	-.1441	-.0986
15.94	.8858	.0563	.0333	.3905	.1305	-.0328	-.0218
15.94	.9682	.0202	-.0168	.3187	.1235	.0215	.0053
15.92	1.0626	-.0297	-.0804	.3028	.1214	.0732	.0294
15.90	1.1665	-.1028	-.1666	.2739	.1165	.1398	.0745
15.90	1.3216	-.2070	-.2911	.2611	.0969	.2044	.1194
15.94	1.4064	-.2754	-.3658	.2475	.0939	.2445	.1444
15.90	1.5088	-.3642	-.4695	.2395	.1114	.2747	.1620
15.95	1.6361	-.4763	-.6002	.2267	.1079	.3068	.1898
15.94	1.7471	-.5850	-.7316	.2343	.1028	.3409	.2069
15.90	1.9116	-.7803	-.9451	.2155	.1071	.3611	.2167
15.90	2.0254	-.9197	-1.0934	.2225	.1110	.4020	.2435
15.95	2.2023	-1.1076	-1.3248	.2254	.1115	.4172	.2522

RUN# 42

ALPHA	J	CP	CT	CPM	CNF	CYM	CSF
19.85	.6648	.1620	.1657	.6167	.2501	-.3649	-.2462
19.80	.7595	.1251	.1180	.5241	.2223	-.1964	-.1208
19.84	.8839	.0693	.0506	.4507	.1886	-.0611	-.0378
19.85	.9649	.0345	.0030	.4077	.1690	-.0076	-.0132
19.85	1.0587	-.0165	-.0591	.3743	.1613	.0437	.0001
19.80	1.1769	-.0822	-.1472	.3610	.1615	.1243	.0439
19.84	1.3297	-.1800	-.2636	.3162	.1410	.1804	.0794
19.84	1.4118	-.2407	-.3378	.3086	.1399	.2080	.0914
19.85	1.5072	-.3278	-.4252	.2920	.1364	.2425	.1210
19.85	1.6366	-.4278	-.5598	.2911	.1285	.2886	.1415
19.80	1.7697	-.5603	-.7314	.2792	.1272	.3324	.1740
19.84	1.8913	-.7012	-.8570	.2924	.1406	.3511	.1795
19.84	2.0392	-.8302	-1.0526	.2660	.1333	.3751	.1955
19.80	2.1969	-1.0634	-1.2901	.3036	.1459	.3776	.1873

RUN# 44

ALPHA	J	CP	CT	CPM	CNF	CYM	CSF
.12	.6657	.0195	-.2082	.0111	.0386	-.0052	.0007
.10	.7608	.0224	-.2709	.0321	.0534	-.0233	-.0077
.08	.8863	.0202	-.3661	.0084	.0377	-.0209	-.0070
.10	.9642	.0173	-.4328	-.0070	.0346	.0187	.0188
.06	1.0660	.0138	-.5257	-.0031	.0263	.0076	.0105
.06	1.1795	.0158	-.6452	.0008	.0271	-.0030	.0049
.10	1.3297	.0123	-.8054	-.0046	.0434	-.0144	-.0063
.10	1.4159	.0137	-.9127	-.0191	.0307	-.0037	.0051
.12	1.5082	-.0004	-1.0143	.0036	.0471	.0050	.0081
.10	1.6530	-.0117	-1.2086	.0047	.0461	-.0150	-.0003
.12	1.7703	-.0137	-1.3736	.0048	.0378	-.0065	.0026
.04	1.9044	-.0277	-1.5848	-.0163	.0495	-.0129	.0082
.06	2.0470	-.0205	-1.7702	.0061	.0380	-.0069	.0083
.06	2.2132	-.0519	-2.0458	.0087	.0385	-.0138	-.0140

TABLE CII. Continued

RUN= 50

ALPHA	J	CP	CT	CPM	CNF	CYM	CSF
-.12	1.2021	.9741	.4791	.0091	.0345	-.0373	.0007
-.10	1.3374	.8669	.4294	.0151	.0399	-.0342	.0055
-.14	1.4538	.7416	.3619	.0233	.0535	-.0231	.0077
-.12	1.5976	.6190	.2869	.0264	.0386	-.0367	-.0071
-.14	1.7140	.4896	.2237	.0162	.0370	-.0257	-.0014
-.10	1.7913	.4015	.1851	.0268	.0501	-.0141	.0085

RUN= 51

ALPHA	J	CP	CT	CPM	CNF	CYM	CSF
8.01	1.2023	1.0052	.5011	.4251	.2206	-.1721	-.1266
7.97	1.3350	.8881	.4428	.3837	.1958	-.1188	-.0770
7.97	1.4120	.8179	.4084	.3752	.2135	-.0923	-.0599
8.01	1.6143	.6331	.3171	.3375	.1976	-.0199	-.0032
7.99	1.6504	.5996	.2914	.3449	.1913	-.0428	-.0109
8.01	1.7771	.4666	.2205	.3252	.1795	.0009	.0176
7.99	1.9129	.3287	.1546	.3199	.1692	.0241	.0250
7.97	2.0543	.1564	.0607	.3094	.1871	.0373	.0442
7.97	2.2278	-.0790	-.0520	.3182	.1815	.0524	.0572

RUN= 52

ALPHA	J	CP	CT	CPM	CNF	CYM	CSF
15.95	1.3375	.9574	.4788	.7607	.3893	-.2045	-.1448
15.99	1.4218	.8850	.4476	.7287	.3897	-.1767	-.1238
15.99	1.5168	.7988	.4009	.7053	.3699	-.1351	-.0874
15.97	1.6564	.6710	.3388	.6679	.3540	-.0686	-.0334
15.97	1.8034	.5417	.2665	.6347	.3381	-.0132	.0034
15.95	1.8887	.4420	.2230	.6211	.3190	.0211	.0278
15.97	2.0658	.2506	.1350	.5786	.2983	.0761	.0607
15.99	2.2202	.0990	.0510	.5839	.2924	.1155	.0929

RUN= 53

ALPHA	J	CP	CT	CPM	CNF	CYM	CSF
19.76	1.4082	.9495	.4820	.9351	.4898	-.2237	-.1386
19.74	1.5306	.8487	.4285	.8805	.4678	-.1541	-.0863
19.70	1.6433	.7542	.3800	.8331	.4436	-.0985	-.0503
19.70	1.7713	.6477	.3229	.7831	.4132	-.0206	.0061
19.70	1.8986	.5340	.2637	.7752	.3955	.0003	.0200
19.76	2.0531	.3773	.1943	.7330	.3748	.0616	.0530
19.70	2.2197	.1920	.0996	.7077	.3706	.1117	.0830

TABLE CII. Concluded

RUN= 85

ALPHA	J	CP	CT	CPM	CNF	CYM	CSF
-.05	.6824	.2961	.2649	.0030	.0066	-.0329	-.0142
-.05	.7705	.2504	.2163	.0012	.0105	-.0219	-.0084
-.05	.9039	.1709	.1408	.0084	.0164	-.0105	-.0084
-.05	.9810	.1211	.0949	.0061	.0173	-.0097	-.0051
-.05	1.0813	.0529	.0329	.0077	.0192	-.0072	-.0048
-.05	1.1830	-.0161	-.0383	.0013	.0004	-.0056	-.0052
-.05	1.3408	-.1397	-.1542	.0267	.0182	-.0026	.0001
-.05	1.4263	-.2227	-.2264	.0161	-.0026	-.0041	-.0041
-.05	1.5319	-.3408	-.3268	.0123	.0241	-.0039	-.0001
-.05	1.6556	-.4699	-.4573	.0177	.0355	.0063	.0008
-.03	1.7788	-.6250	-.5921	.0140	-.0005	.0155	.0121
-.03	1.9167	-.8636	-.7717	.0193	.0195	.0145	.0042
-.05	2.1148	-1.1372	-1.0583	.0377	.0161	.0087	-.0004
-.05	2.4552	-1.6790	-1.5849	.0176	.0136	.0176	.0105
-.03	2.2545	-1.3664	-1.2677	-.0017			

RUN= 87

ALPHA	J	CP	CT	CPM	CNF	CYM	CSF
8.12	.6816	.2988	.2707	.3000	.0924	-.2422	-.2045
8.12	.7707	.2528	.2236	.2627	.1061	-.1584	-.1325
8.12	.8943	.1781	.1537	.2315	.1119	-.0721	-.0575
8.12	.9871	.1381	.1031	.2279	.1217	-.0302	-.0262
8.12	1.0764	.0666	.0451	.2013	.0812	.0075	.0080
8.12	1.1884	-.0070	-.0282	.1888	.0889	.0508	.0411
8.12	1.3466	-.1408	-.1473	.1856	.0906	.1029	.0748
8.12	1.4335	-.2253	-.2200	.1792	.0810	.1253	.0935
8.12	1.5366	-.3289	-.3117	.1706	.0887	.1560	.1080
8.12	1.6777	-.4818	-.4582	.1622	.0696	.1079	.1394
8.12	1.7976	-.6030	-.5842	.1570	.0962	.2158	.1546
8.12	1.9380	-.8048	-.7663	.1548	.0703	.2570	.1924
8.12	2.0720	-.7743	-.9438	.1512	.0433	.2902	.2127
8.12	2.2327	-1.2422	-1.1763	.1543	.0907	.3300	.2356

RUN= 88

ALPHA	J	CP	CT	CPM	CNF	CYM	CSF
16.07	.6752	.3171	.2698	.6487	.3012	-.4546	-.3550
16.07	.7674	.2674	.2426	.5694	.2601	-.3060	-.2266
16.05	.8937	.2016	.1760	.4825	.2429	-.1465	-.1118
16.05	.9764	.1508	.1283	.4440	.2083	-.0700	-.0515
16.05	1.0796	.1033	.0690	.3990	.2069	.0070	-.0009
16.05	1.1882	.0177	.0039	.3790	.1586	.0623	.0276
16.05	1.3454	-.1027	-.1089	.3553	.1819	.1432	.0746
16.05	1.4363	-.1696	-.1734	.3417	.1712	.1790	.1020
16.03	1.5713	-.3226	-.3036	.3322	.1704	.2399	.1472
16.05	1.6719	-.4150	-.3834	.3197	.1679	.2645	.1628
16.05	1.7865	-.5479	-.4895	.3162	.1587	.3038	.1840
16.05	1.9121	-.7219	-.6443	.3087	.1494	.3329	.2014
16.03	2.0790	-.9221	-.8301	.3110	.1687	.3684	.2160
16.05	2.2395	-1.1569	-1.0443	.3056	.1778	.3993	.2333

1. Report No. NASA TM-86364	2. Government Accession No.	3. Recipient's Catalog No.	
4. Title and Subtitle Low-Speed Wind-Tunnel Tests of an Advanced Eight-Bladed Propeller		5. Report Date July 1985	
7. Author(s) Paul L. Coe, Jr., Garl L. Gentry, Jr., and Dana Morris Dunham		6. Performing Organization Code 535-03-12-07	
9. Performing Organization Name and Address NASA Langley Research Center Hampton, VA 23665		8. Performing Organization Report No. L-15898	
12. Sponsoring Agency Name and Address National Aeronautics and Space Administration Washington, DC 20546		10. Work Unit No.	
		11. Contract or Grant No.	
		13. Type of Report and Period Covered Technical Memorandum	
		14. Sponsoring Agency Code	
15. Supplementary Notes			
16. Abstract As part of a research program on advanced turboprop aircraft aerodynamics, a low-speed wind-tunnel investigation was conducted to document the basic performance and force and moment characteristics of an advanced eight-bladed propeller. The results show that in addition to the normal force and pitching moment produced by the propeller/nacelle combination at angle of attack, a significant side force and yawing moment are also produced. Furthermore, it is shown that for test conditions wherein compressibility effects can be ignored, accurate simulation of propeller performance and flow fields can be achieved by matching the nondimensional power loading of the model propeller to that of the full-scale propeller.			
17. Key Words (Suggested by Author(s)) Turboprops Propeller nacelle Aircraft stability and control		18. Distribution Statement Unclassified—Unlimited	
Subject Categories 02, 08			
19. Security Classif.(of this report) Unclassified	20. Security Classif.(of this page) Unclassified	21. No. of Pages 47	22. Price A03

For sale by the National Technical Information Service, Springfield, Virginia 22161

NASA-Langley, 1985